[redacted]

[redacted]

Total No. of Pages 100

Copy No [redacted]

REPORT NO. 8

KH-4B SYSTEM CAPABILITY

Evaluation of SO-242 Film for Use With the KH-4B System

4 AUGUST 1970

Authors: [redacted]

[redacted]

HANDLE VIA
~~TALENT-KEYHOLE~~
CONTROL SYSTEM ONLY

Notice of Missing Page(s)

Pages 12, 14, 38, 44, and 46 of the original document apparently were considered parts of oversize pages and were not given separate page numbers.

This page intentionally blank.

CONTENTS

FIGURES

TABLES

1. HISTORICAL PERSPECTIVE

Mission 1108 was launched on 4 December 1969 and recovered on 21 December during rev 276. As an experiment, 819 feet of SO-242 Aerial Color Film were included as a tag-on to the aft-looking camera film supply. Color coverage was obtained on 13 photographic passes and totalled 213 frames.

Previous missions in this series had acquired color information in various modes on a limited basis. Early KH-4B camera pairs utilized green filter acquisition to complement red filter acquisition on 3404 (black and white) film to provide synthesis of bi-color imagery* with ground handling equipment. Registration difficulties, minimal color cues, and the advent of high resolution color film have since discouraged further use of the bi-color technique on the KH-4B system. Color translation was experimented with on mission 1104-2 by acquiring imagery on SO-180 Infrared Ektachrome Film.† Near-infrared-sensitive layer speed instability, electrostatic discharge fogging, and approximately 30-foot optimum ground resolution performance level have impeded further use of this color approach. An improved version of this material would have a high potential in the KH-4B system. Natural color was acquired with SO-121 Aero Ektachrome film tag-ons to missions 1105-2 and 1106-2 with promising results.‡ There was a film curl anomaly on 1105 and a film separation anomaly on 1106, but capability was demonstrated at a 25-foot optimum ground resolution level.

The improved Aerial Color Film, SO-242, in the system is free of any serious anomalies and has demonstrated both better color discrimination and a 15-foot ground resolution optimum performance level. This document reports the results of the special engineering operations with SO-242 film in the KH-4B system. The objectives established and met for this test were: (1) to obtain improved conventional color photography with the KH-4B system: (2) to demonstrate the in-flight characteristics of SO-242 film in the KH-4B cameras; and (3) to certify operational capability.

---

*CR-2 Bi-Color Experiment [redacted] (27 Sept 1968). Special Purpose Photographic Techniques for Overhead Reconnaissance, [redacted] Oct 1969).

†Evaluation of SO-180 Film for Use With the KH-4B System. [redacted] 4 Aug 1969).

‡Evaluation of SO-121 Film for Use With the KH-4B System. [redacted] (20 Nov 1969).

This page intentionally blank.

2. TEST DESCRIPTION

The CR-9 aft-looking camera (unit no. 316 with second generation Petzval lens I-169) returned 7,088 feet of 3404 film plus 819 feet of SO-242 Aerial Color Film as a tag-on. All of this 3404 film was exposed through a Wratten no. 21 filter in the primary position. A material change detection (MCD) system switched the filter to its alternate position when the SO-242 material entered the active exposure mode. In the alternate position was a Wratten no. 2B filter. Because SO-242 is autonomously filtered within its own structure, the Wratten no. 2B filter was required only to maintain the focal setting of the lens, and affected the film's spectral response imperceptibly. Additionally, however, the Wratten no. 2B filter did provide a contingency safety factor for filtering out at least the most degrading blue light in the chance event of the alternate filter being called into place accidentally with the 3404 film. Photographic speed of the SO-242 is comparable to that of the black and white film, such that the given array of slit widths was adequate to cover most of the dynamic exposure range encountered on the mission for both films.

Color coverage was obtained on 13 photographic passes (213 frames) as indicated on Figs. 2-1 and 2-2. The SO-242 color portion began on frame 28 of rev D-242 (as the vehicle passed over southwest USA) and continued to the end of the mission, frame 2 of rev D-274 (over northern Texas). Processing of original SO-242 positives and production of duplicate SO-360 (Aerial Color Duplicating Film) positives were carried out at [redacted]

All of the passes using the color film were accomplished in the stereo mode. With 3404 film and a Wratten no. 25 filter in the forward-looking camera (unit no. 317 with third generation Petzval lens I-209), high resolution comparative coverage was obtained for most of the SO-242 frames, with the usual six-frame differential between the two cameras.

Although 51/51 T-bar, 100-foot edge, five-step gray scale and tri-color targets had been deployed for color imagery, acquisition of these deployments was unsuccessful. Ground resolution therefore had to be estimated indirectly, with the result that the sharpest color imagery produced about a 15-foot resolution level. The stereo pair 3404 original negatives produced about a 7-foot ground resolution, which is roughly a 2× difference in performance level from the SO-242 original positives. Working with dupes from both the black and white and color records, there is no difficulty in doing stereo analysis.

The first evaluation of the color imagery (at the processing site) appeared in the mission 1108-2 [redacted] message*:

> "BALANCE AND COLOR SATURATION IS CONSIDERED GOOD. THE BEST GROUND RESOLUTION OF THE SO-242 FROM THIS MISSION APPEARS COMPARABLE TO THE BEST COLOR PROVIDED BY MISSION 1106. ALTHOUGH THE OVERALL COLOR BALANCE IS

---

* [redacted] message no [redacted] 24 Dec 1969.

GOOD AND SLIGHT SHIFT TOWARD CYAN IS APPARENT ON SOME PASSES, THE DENSITY RANGES FROM GENERALLY MEDIUM TO SLIGHTLY HEAVY.

DEGRADATIONS TO THE COLOR MATERIAL ARE MINOR; HOWEVER, SEVERAL BLUISH COLORED MARKS ARE PRESENT INTERMITTENTLY THROUGHOUT THE MISSION. REPETITIVE SMALL YELLOW SPOTS ARE PRESENT 3.1 INCHES APART AND 1.2 INCHES FROM THE CAMERA NUMBER EDGE THROUGHOUT THE COLOR MATERIAL. THE LAST FOUR FRAMES OF THE MATERIAL CONTAIN CREASES AND ABRASIONS ASSOCIATED WITH FILM WRAP UP (i.e., depletion)."

The mission 1108 PET studied the product and produced the following PEIR message*:

"EARLY EVALUATIONS OF THE COLOR MATERIAL FROM THIS MISSION WERE CONDUCTED FROM THE COLOR DUPES AND THE RESULTING COMMENTS WERE GENERALLY NEGATIVE. THE PHOTOINTERPRETERS REPORTED THE PI SUITABILITY OF THE COLOR RECORD AS POOR FOR FIRST PHASE EVALUATIONS BECAUSE OF THE SMALL SCALE AND LOWER RESOLUTION LEVELS. THE PET FELT THAT THE BEST IMAGE QUALITY AND COLOR BALANCE OF THE ORIGINAL SO-242 ARE GOOD, BUT NOTED THAT THERE IS A SIGNIFICANT RESOLUTION LOSS FROM THE ORIGINAL TO THE DUPLICATES. MUCH OF THE SO-242 PHOTOGRAPHY APPEARED TO BE DEGRADED BY HAZE, PARTICULARLY AT THE LOW SOLAR ALTITUDES (LESS THAN 15 DEGREES). THE BEST COLOR IMAGE QUALITY WAS TAKEN AT THE HIGHER SOLAR ALTITUDES (40 DEGREES). THIS COLOR PHOTOGRAPHY IS BETTER THAN ANY OTHER COLOR PHOTOGRAPHY OBTAINED TO DATE FROM THE . . . SYSTEM, EVEN THOUGH THIS FLIGHT WAS FLOWN AT 15 PER CENT HIGHER ALTITUDE. PARTICULARLY NOTABLE WAS THE FINER DYE STRUCTURE OF THE SO-242 MATERIAL WHEN COMPARED WITH SO-121. ELECTROSTATIC FOGGING DOES NOT APPEAR TO BE A PROBLEM WITH SO-242 IN THE . . . SYSTEM."

*NPIC message no. [redacted] 19 Jan 1970.

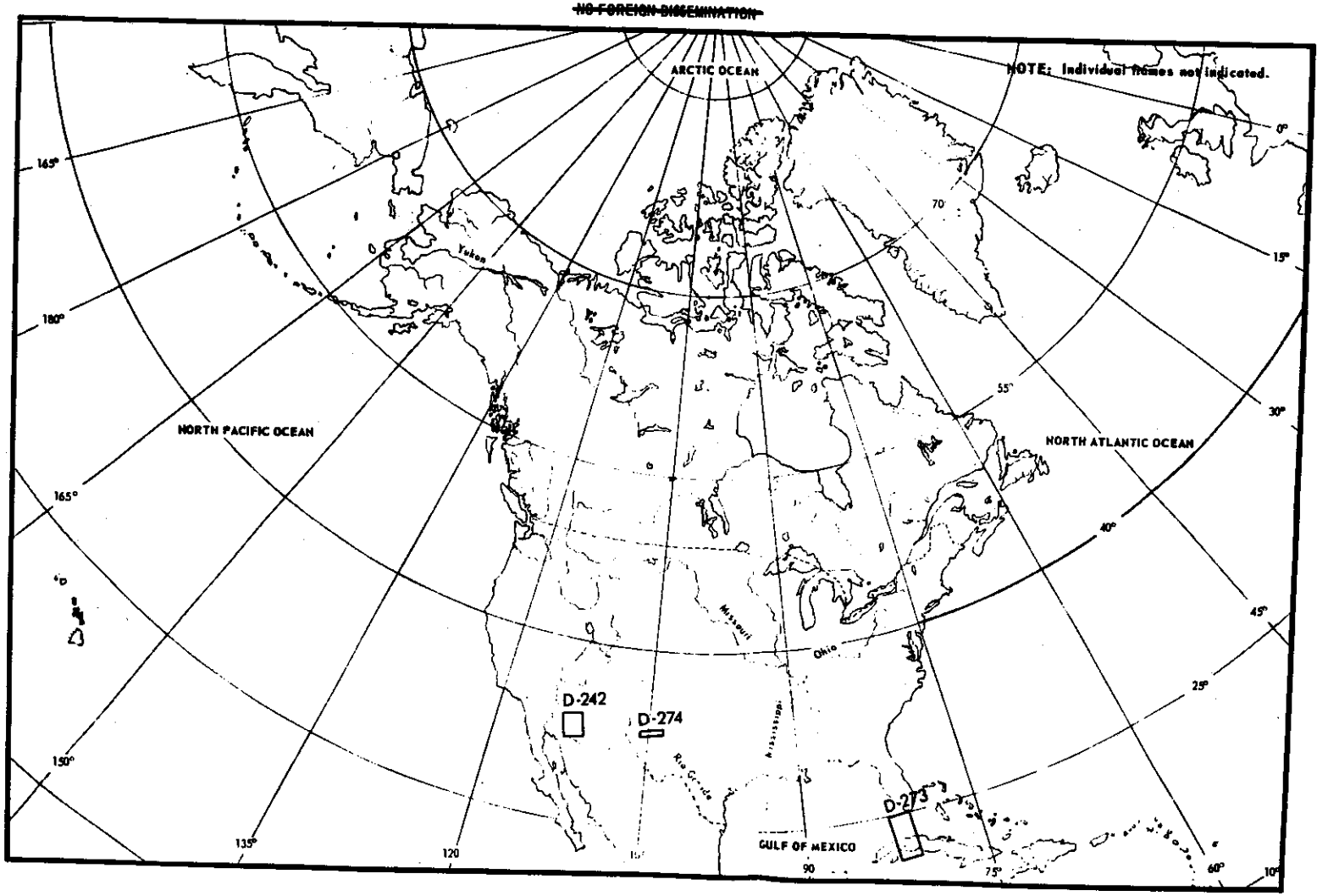

Fig. 2-1 — Ground tracks for mission 1108 SO-242 passes over the United States and Cuba

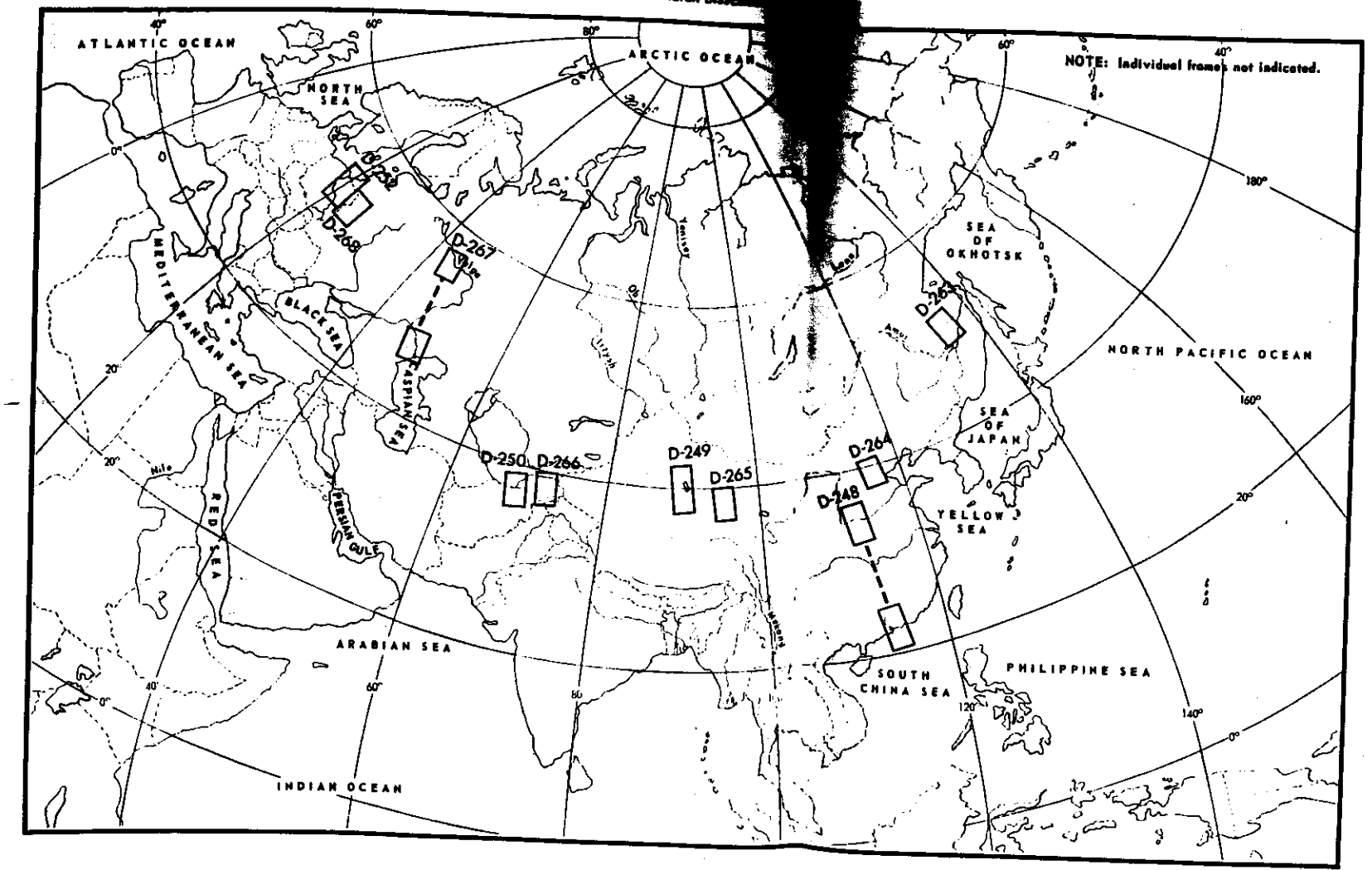

Fig. 2-2 — Ground tracks for mission 1108 SO-242 passes over Eurasia

3. CHARACTERISTICS OF SO-242 FILM

3.1 PHYSICAL STRUCTURE

SO-242 film is an Ektachrome type emulsion on Estar thin base. The film's physical structure, illustrated in Figs. 3-1 and 3-2, accrues three sensitive layers supported by a polyester (thin) base made from polyethylene terephthalate. The ultrathin base counterpart to this film is identified as SO-255.

The three sensitive layers of silver halide suspended in gelatin of slightly different thicknesses, along with their ancillary layers, occupy a total displacement of 0.0008 inch. For anticurl provision, a clear 0.0005-inch-thick gelatin backing is included in the structure. With a base thickness of 0.0025 inch, the total thickness of SO-242 thus amounts to an average of 0.0038 inch. Variations of 0.0001 inch are within limits established by quality control during manufacture, although additional variations of less severity are introduced by fluctuations in moisture content resulting from changes in temperature and relative humidity.

The important point is that the SO-242 color film is 0.0008 inch thicker than the 3404 black and white film. Because of this thickness difference, the film supply footage for the camera employing SO-242, full or in part, must be less than the other camera employing a full load of 3404. In the case of mission 1108, the forward-looking unit, 317, was supplied with 16,300 feet of 3404 while the aft-looking unit, 316, was supplied with 15,200 feet of 3404 and 800 feet of SO-242, resulting in 300 feet less total film footage. Utilization of the SO-255 (UTB) film in place of SO-242 would cancel this camera footage supply difference. For equal amounts of spool displacement, SO-242 footage is about 80 percent of the 3404 footage while the SO-255 footage is about 10 percent more than the 3404 footage. These observations regarding footage advantages of SO-255 (UTB tri-pack) over SO-242 (STB tri-pack) are to be qualified by the fact that the KH-4B system capability with SO-255 film has not yet been demonstrated. Considering the incompatibility of SO-380 (UTB monolayer) in the film transport mechanism of the cameras, responsible testing of the color UTB in the system would be necessary.

Image forming energy incident onto SO-242 is filtered by a Wratten no. 2B equivalent coating and then penetrates into the green sensitive, red sensitive, and blue sensitive layers, respectively (Figs. 3-1 and 3-2). The integral filtration removes the shortest wavelengths of light to which all three layers are sensitive. This arrangement of layers is different from that of either the SO-121 or SO-180 films used in previous KH-4B experiments. A comparison of the layer orientations of these three film types is given in Table 3-1. For image quality reasons revealed in Section 4, the "ideal" color film for use in the KH-4B system would have its red sensitive layer on top, followed by the green, and then yellow sensitive layers. This mythical film is included in Table 3-1 to draw the comparison out to its logical extension.

Whereas both SO-180 and SO-121 require supplementary spectral filtration, SO-242 is characterized by integral filtration. One advantage of integral filtration is a reduction in sensitivity

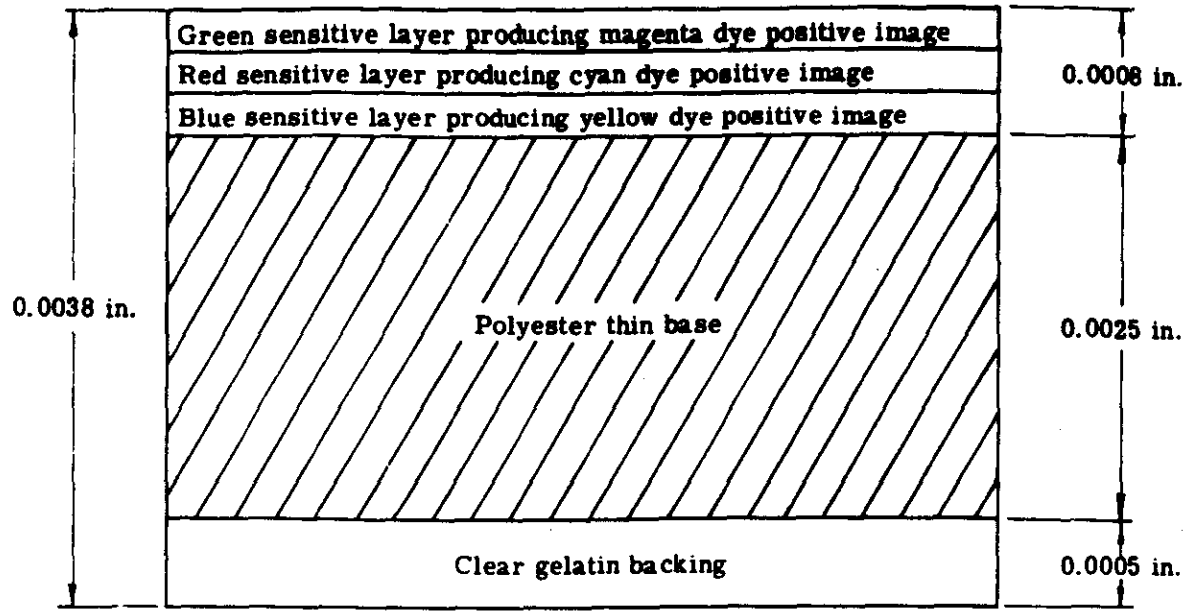

(a) SO-242 film

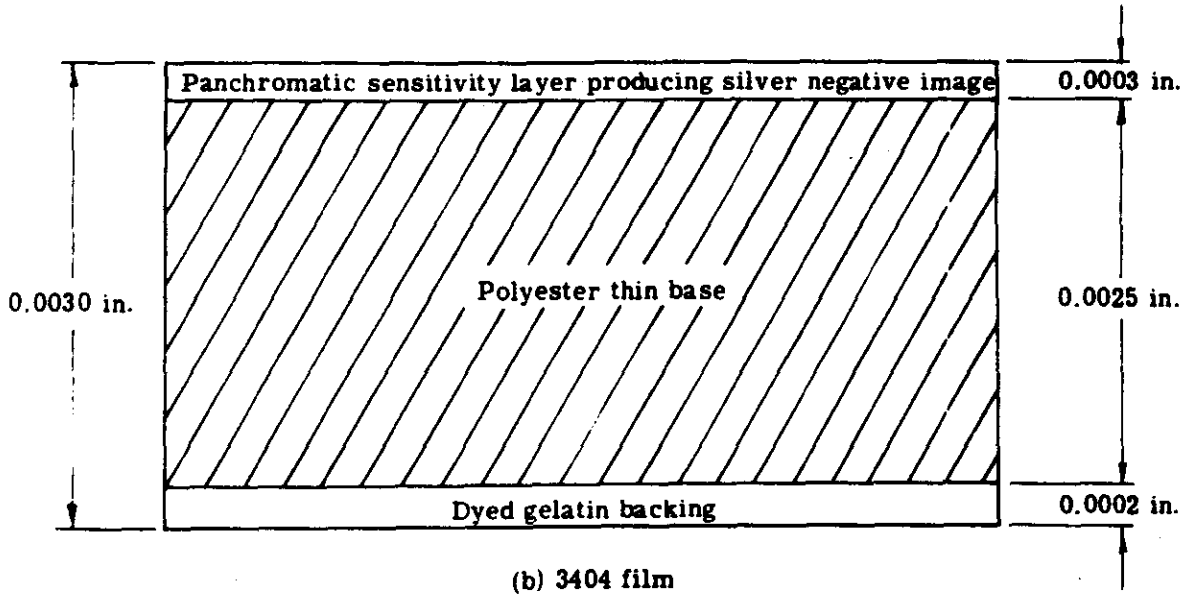

(b) 3404 film

Fig. 3-1 — Physical structure of SO-242 and 3404 films

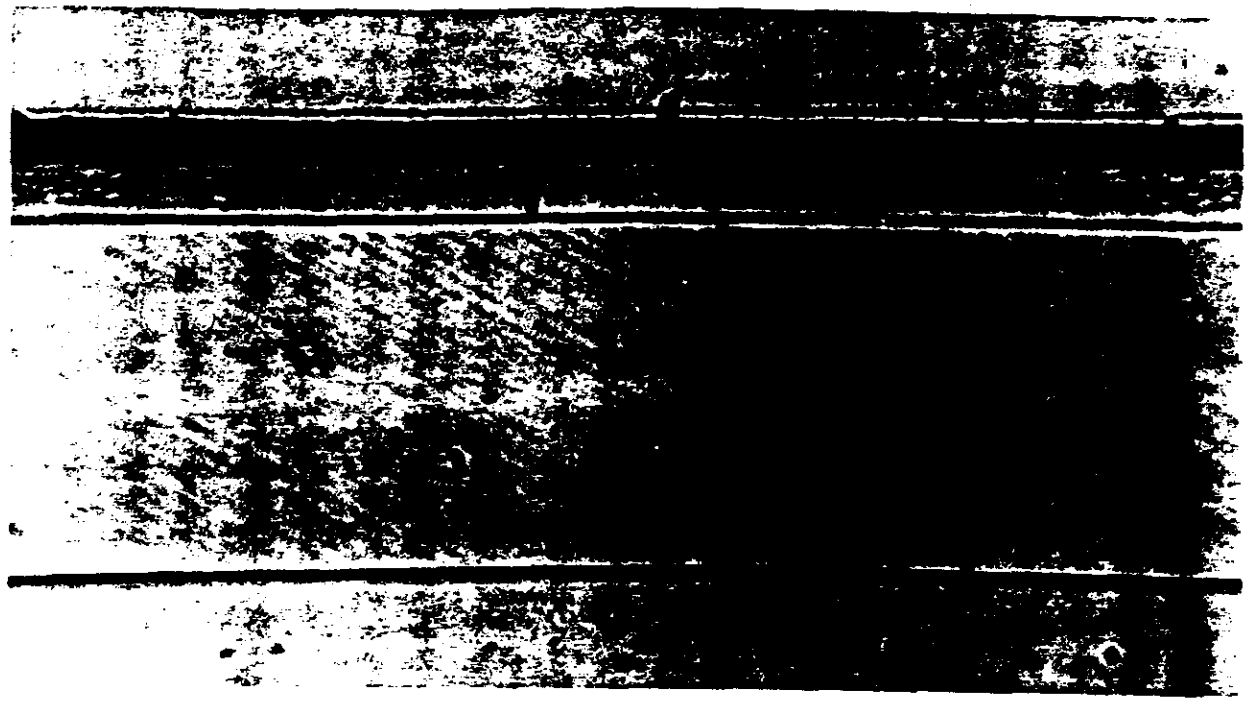

(a) SO-242 film

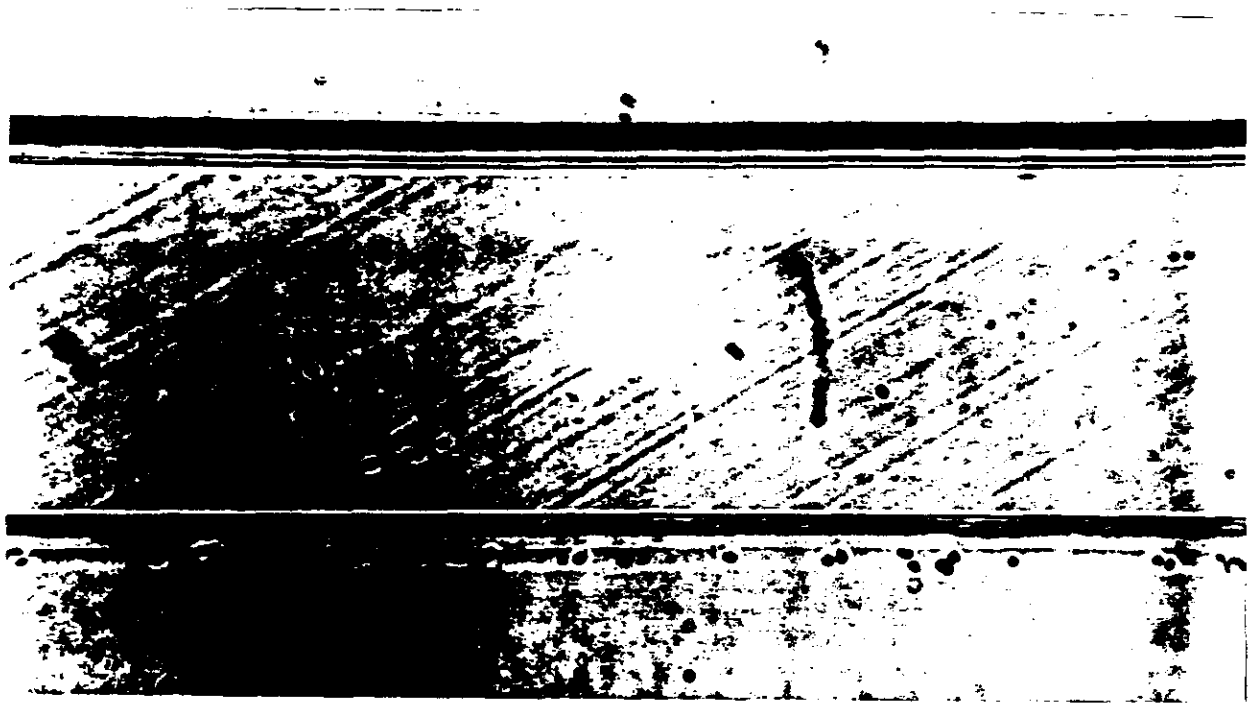

(b) 3404 film

Fig. 3-2 — 700× photomicrographs of cross sections of SO-242 and 3404 films

This page intentionally blank.

Table 3-1 — Layer Orientations of the Three Color Films Used in KH-4B Experiments

NOTE: [ ] indicates apart from film's structure
( ) indicates requirement for tag-ons only

Film	Orientation
SO-180	Incident light [Wratten no. 15 (+ND)] 1. Near infrared 2. Green 3. Red Base Backing
SO-121	Incident light [Wratten no. 2E + CC (+ND)] 1. Green 2. Blue 3. Red Base Backing
SO-242	Incident light [(Wratten no. 2B)] 0. Wratten no. 2B 1. Green 2. Red 3. Blue Base Backing
KH-4B "ideal"	Incident light 0. Filter 1. Red 2. Green 3. Blue Base Backing

to electrostatic discharge fogging during transport in KH-4B cameras, but the extent of this advantage has not been tested.

For gelatin filter KH-4B systems, use of the SO-180 and SO-121 films had to be anticipated with rather "last minute" synthesis of Wratten no. 15 plus neutral density or Wratten no. 2E plus color compensation plus neutral density filters, the transmission specifications for which were defined by the expected orbital parameters of the 1104, 1105, and 1106 missions. Now that glass filter KH-4B systems are phasing in, tailored filtration is untenable. Glass filter substrates treated with vacuum deposited dichroic interference layers have been prepared for use with integral filter color films: SO-242 (color rendition) and 3443* (color translation). These glass filters are 0.040 inch thick and will be used to maintain focal position when the alternate filter position is elected. Wratten nos. 25, 23A, and 21 type dichroic coatings on 0.040-inch substrate are available for installation in the primary filter positions. The singular purpose of the color film filters is for safety. In the event that the alternate filter position is called into place accidentally, the most detrimental short wavelengths of scattered light will be filtered out to somewhat preserve contrast and proper exposure on the black and white film, which would not be so with just clear glass.

3.2 PHOTOGRAPHIC SENSITIVITY

In order to determine the spectral sensitivity of the three recording layers composing SO-242, sample strips were exposed on an equal energy spectrosensitometer. A processed film spectrogram is reproduced in Fig. 3-3 to illustrate the film's spectral response. This reproduction is given for graphic illustration only, and does not perfectly represent the spectral information of the SO-242 transparency film. A point within the exposed area is referenced by a particular wavelength (from 400 to 700 nanometers) along the x axis and by a log exposure value (in 10 levels) along the y axis. The fact that the exposing unit is an equal energy source for the wavelength region considered allows a straightforward conversion from measured density through effective exposure to the specification of absolute spectral sensitivity. Spectral sensitivity is defined here as the reciprocal of the energy necessary to produce an analytical filter density of unity.

The SO-242 spectrogram was traced on a Mann microdensitometer to obtain integral filter density readings as a function of wavelength and exposure level. An 80-micron spot aperture was used to cover the equivalent of about 1/4-nanometer wavelength increment on the spectrogram. A total of 24 tracks were traced through exposure across the spectrogram. For each track, density was measured with respect to blue (440 nanometers), green (540 nanometers), and red (670 nanometers) filtration. Zero was referenced to base plus stain. The resulting measurements are integral filter densities.

To obtain the spectral sensitivities of the three layers independent of one another, the integral filter densities† were converted to analytical filter densities, such that the interaction of the dyes was eliminated for the remainder of the data processing. Yellow, magenta, and cyan analytical filter densities were then plotted as a function of log exposure. Because the 1.0 density level was chosen as the level for which reciprocal energy would be determined, interpolation was performed

---

*Kodak 3443 film is an improved version of SO-180. The 3443 film has better cyan layer speed stability with aging and moisture depletion.

†The terms "analytical filter density" (AFD) and "analytical spectral density" (ASD) are used to distinguish between measurements made with narrow band spectral filters and those made with a spectrophotometer, respectively.

on these curves to produce a log exposure value for yellow, magenta, and cyan at each of the 24 wavelengths sampled microdensitometrically. This data was then antilogged for exposure determination. The reciprocal of the exposing energy was computed for all of the determinations producing sensitivity contours for each of the three sensitive layers. A normalized version of this data is offered in Fig. 3-4 as a comparison to the spectrogram in Fig. 3-3. The absolute response data is plotted in Fig. 3-5. Sensitivity peak locations for the three layers are:

Blue = 440 nanometers
Green = 555 nanometers
Red = 655 nanometers

Comparison of SO-242 spectral sensitivity with that of its predecessor, SO-121, is offered in Fig. 3-6. The red (cyan layer) sensitivities are essentially equivalent, and the shift of the SO-242 blue (yellow layer) sensitivity towards the longer wavelengths from where it is with the SO-121 constitutes only an insignificant gain in lens modulation transfer characteristics during image formation. However, the SO-242 green (magenta layer) sensitivity is free of the SO-121 appreciable sensitivity to blue. As pointed out in the SO-121 Capability Report, this dual sensitivity not only incurs a limited blue/green discrimination capability but also results in degraded image quality in that layer due to the poor transfer of spatial frequencies in the blue spectral region. Both of these difficulties are overcome by the more selective green response of the SO-242 film.

For the purpose of determining the spectral transmission characteristics of the dyes in each of the three sensitive layers, it was convenient to fog out two of the layers, leaving the third layer to develop dye in processing to completion. To complement the three different dye layer samples produced in this way, a base-plus-stain sample, with none of the three dyes contained, was also required. Spectrophotometric traces were made of each of the three dye layer samples, with the base-plus-stain sample serving as the zero reference. This is necessary because the transmission of the base plus stain is not neutral over the spectral domain measured (Fig. 3-7). The spectral transmission traces in the 360- to 800-nanometer wavelength domain of the yellow, magenta, and cyan dyes composing SO-242 imagery were converted to density information and normalized. Results are given in Fig. 3-8. Thus, the aerial image chromatic information content incident onto the film is recorded in accordance with the spectral sensitivity of the silver halide layers (Fig. 3-5) and the processed imagery is viewed or printed in accordance with the spectral density of the dye layers (Fig. 3-8).

3.3 RESOLUTION CAPABILITY

A limited amount of testing was carried out on SO-242 film to determine its resolving power under different chromatic conditions. The results of this work are summarized by the Aerial Image Modulation (AIM) curves given in Fig. 3-9. The data for this figure were generated on a resolving power camera, the microscope objective of which introduced essentially no resolution degradation. Contrast reduction introduced by the camera, however, was taken into account such that the modulation of the aerial image presented to the film was defined. Statistical resolution levels of standard tri-bar targets were then determined for an array of incident modulation levels for white light imagery as well as for red, green, and blue imagery produced by the test camera.

The blue AIM curve is decidedly set apart, located at very low resolution levels. The red and green AIM curves have a similar shape, with the red targets being resolved consistently lower than the green targets. These tests also indicate that the green target imagery is statistically equivalent to the white light or neutral colored resolution targets. It is interesting to note the correspondence of these general resolution trends with the physical structure of the SO-242 film.

Uppermost in the tri-pack is the green sensitive layer, with its resolution unimpeded by any intervening scattering medium. Down into the tri-pack is the comparably performing red sensitive layer, with its effective resolution level lowered somewhat because of the disadvantageous location. At the bottom of the tri-pack is the ultralow resolution capability of the blue sensitive layer.

The physical sensitometric and resolution characteristics of SO-242 film described in this chapter are applied to the KH-4B camera system in the following section.

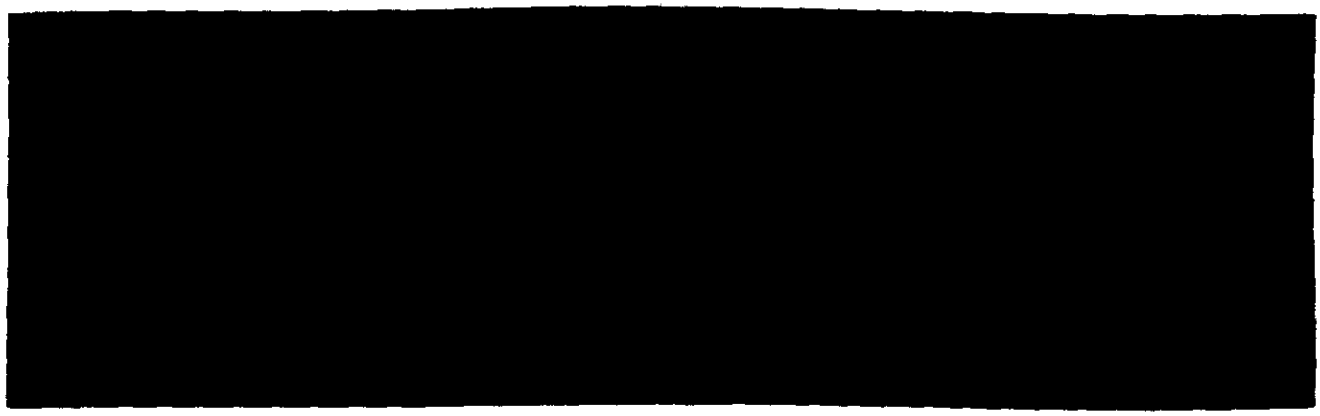

Fig. 3-3 — Reproduction of SO-242 spectrogram

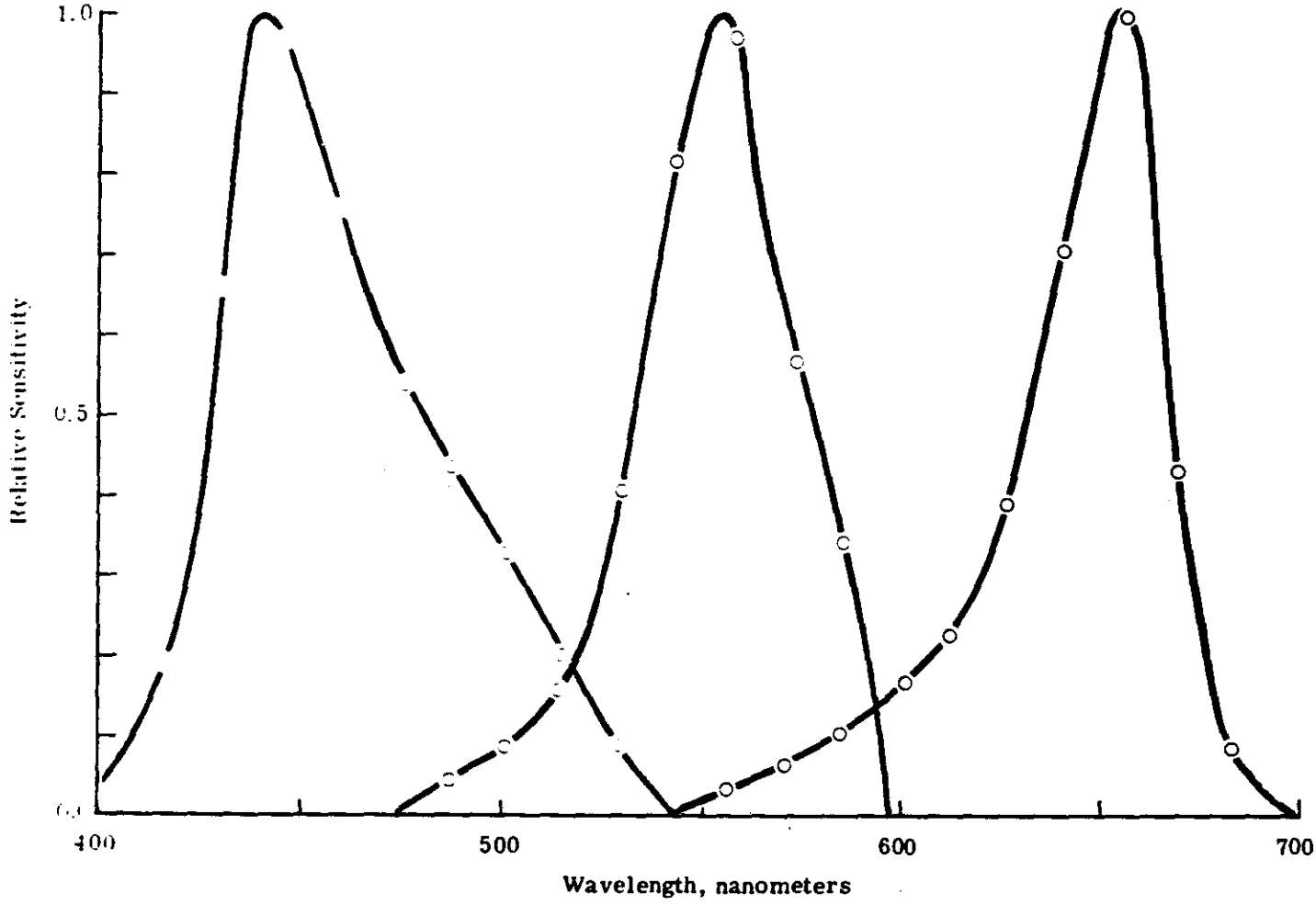

Fig. 3-4 — Spectral sensitivity of SO-242 film

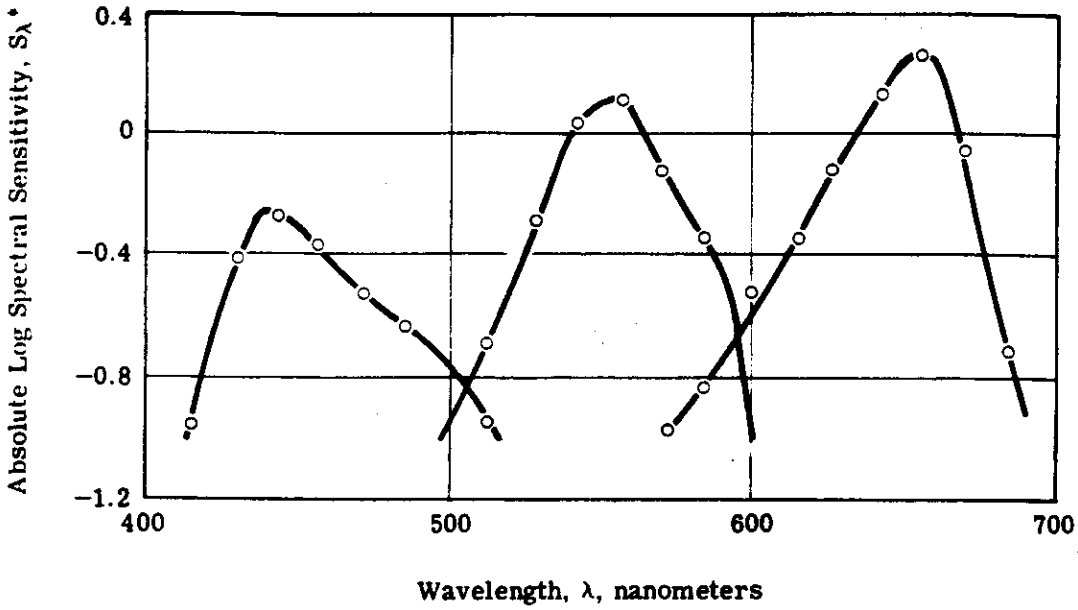

Fig. 3-5 — Absolute spectral sensitivity of SO-242 film

*$S_\lambda = 1/E_\lambda$, where E_λ is energy (ergs/cm^2) of monochromatic light of wavelength, λ, required to reduce the dye image density in individual dye layers to an equivalent neutral density of 1.0 above minimum density.

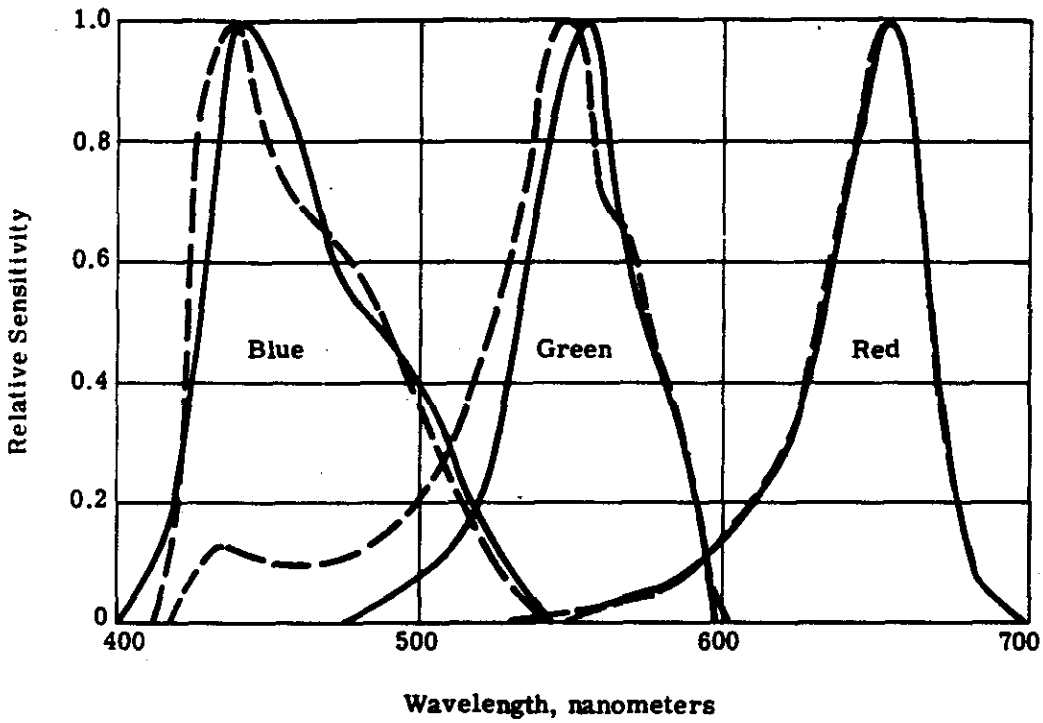

Fig. 3-6 — Normalized spectral sensitivities of SO-242 film filtered with a Wratten no. 2B and SO-121 film filtered with a Wratten no. 2E

——— SO-242 (in-house determination) with external Wratten no. 2B filtration

— — — SO-121 (manufacturer's determination) with external Wratten no. 2E filtration

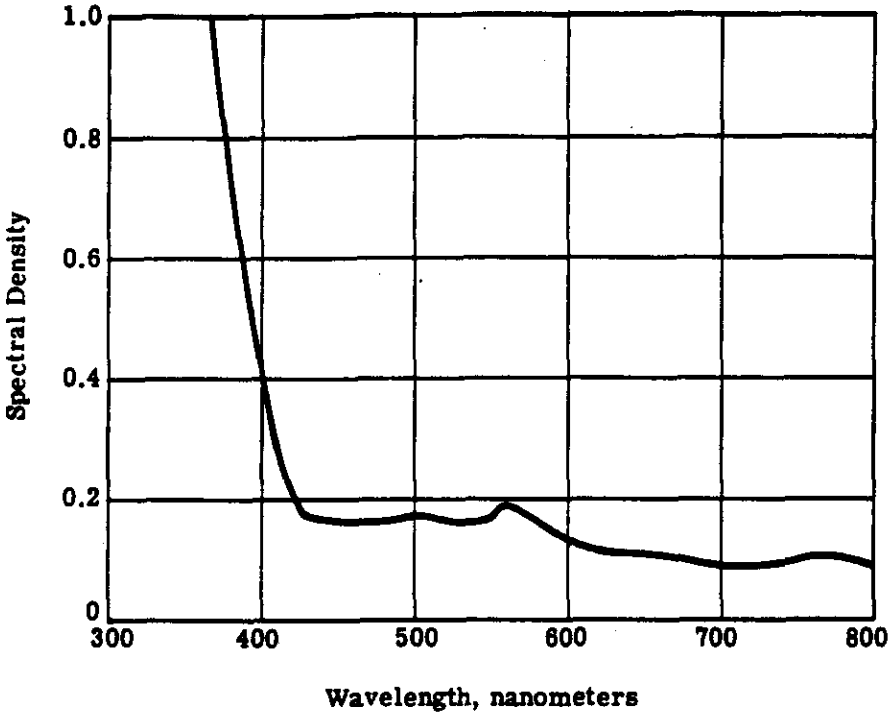

Fig. 3-7 — Spectral density of base-plus-stain of SO-242 film

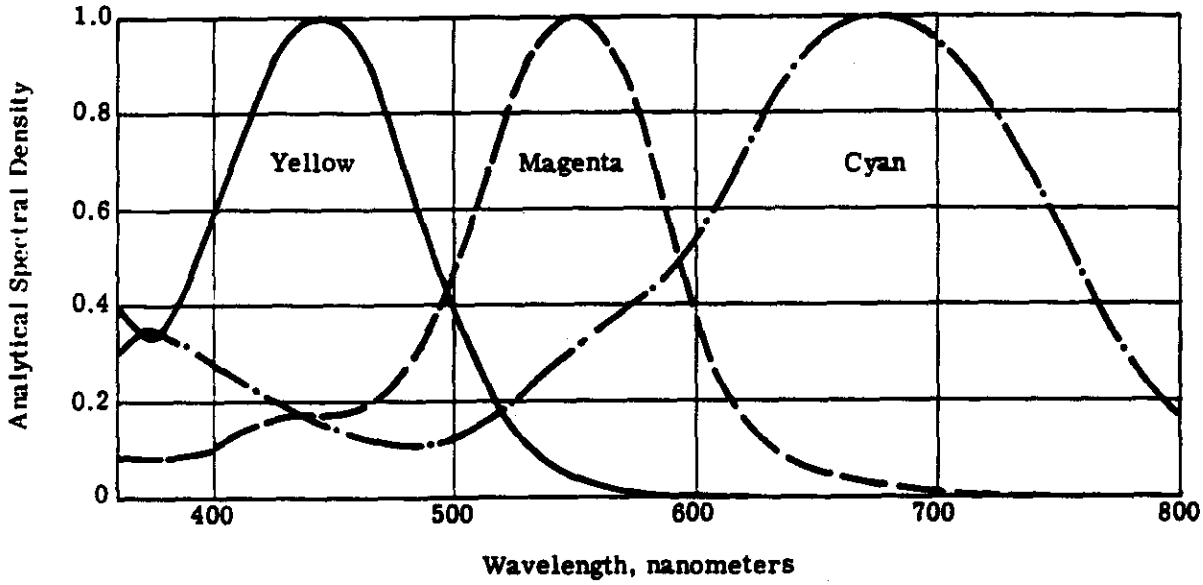

Fig. 3-8 — Dye absorption curves for SO-242 color film

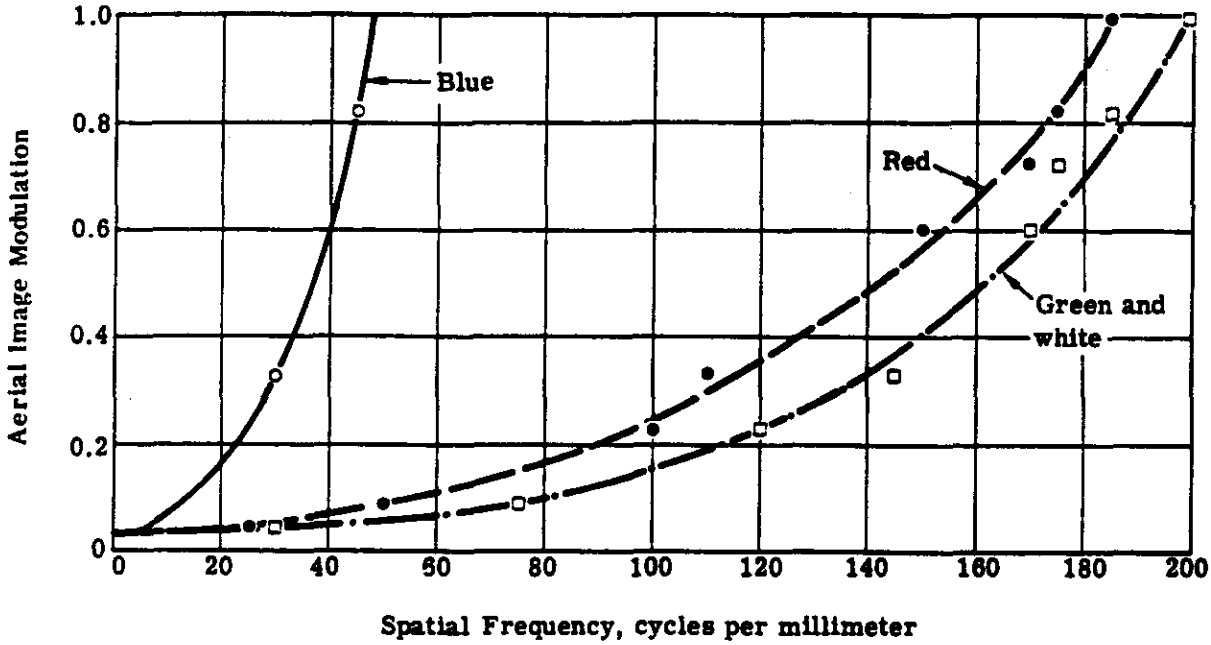

Fig. 3-9 — AIM curves for SO-242 film

4. KH-4B SYSTEM ANALYSIS WITH SO-242 FILM

4.1 PETZVAL LENS MTF's

Modulation transfer functions for second and third generation Petzval lenses are shown in Figs. 4-1 and 4-2.* Fig. 4-1 shows three transfer functions for each generation lens representing the spectrally weighted lens MTF's for the red, green, and blue isolated sensitivities of the SO-242 emulsion layers. Fig. 4-2 shows three transfer functions for each generation lens for monochromatic wavelengths chosen at the peak sensitivities of the three SO-242 layers. In Fig. 4-3 the spectral sensitivities of the three SO-242 layers (as determined in Section 3.2) are shown. The contours superimposed on these spectral sensitivity curves represent modulation transfer as a function of wavelength at two spatial frequencies (10 and 100 cycles per millimeter) for both second and third generation lenses.

Since the blue sensitive response of SO-242 is almost entirely on the outside of these modulation transfer contours, it is evident that the MTF in any portion of this spectral region will be very poor. The green spectral region is more complex. The lens modulation transfer varies through this region such that the spectral composition of the light has an important bearing on the image formation. As a consequence, objects having different green hues will be imaged with different spatial frequency content and therefore different image quality. In the red region, on the other hand, the modulation transfer contours tend to weight the inclusive wavelengths equally. The implication here is that the actual wavelength composition of red objects has much less effect on the final image structure than objects in the green spectral region.

It is also evident from Fig. 4-3 that the second generation lens will perform better than the third generation lens in the green spectral region because modulation transfer values are consistently higher at any wavelength in the 500- to 600-nanometer region. This comparison is also reflected in Figs. 4-1 and 4-2. For red light, this clear-cut distinction is nonexistent. The similarity of the contours in this spectral region tends to result in rather similar performance. However, in Figs. 4-1 and 4-2 the second generation lens is shown to be better at the low spatial frequencies, whereas the third generation lens is shown to be better at the higher spatial frequencies. Because most of the imagery produced in the KH-4B system on SO-242 film is composed of spatial frequencies below 100 cycles per millimeter, the superiority of the second generation lens is suggested.

4.2 SO-242 DYE LAYER ISOLATION

In order to understand what is happening in each of the three emulsion layers of SO-242 the individual cyan, magenta, and yellow dye images must be isolated. A partial isolation can be achieved by viewing the transparency through red, green, or blue separation filters or by printing separate black and white records using the same filters. These procedures produce only a partial

*Note that the blue MTF's in Figs. 4-1 and 4-2 are estimated from geometric considerations based on a defocus condition.

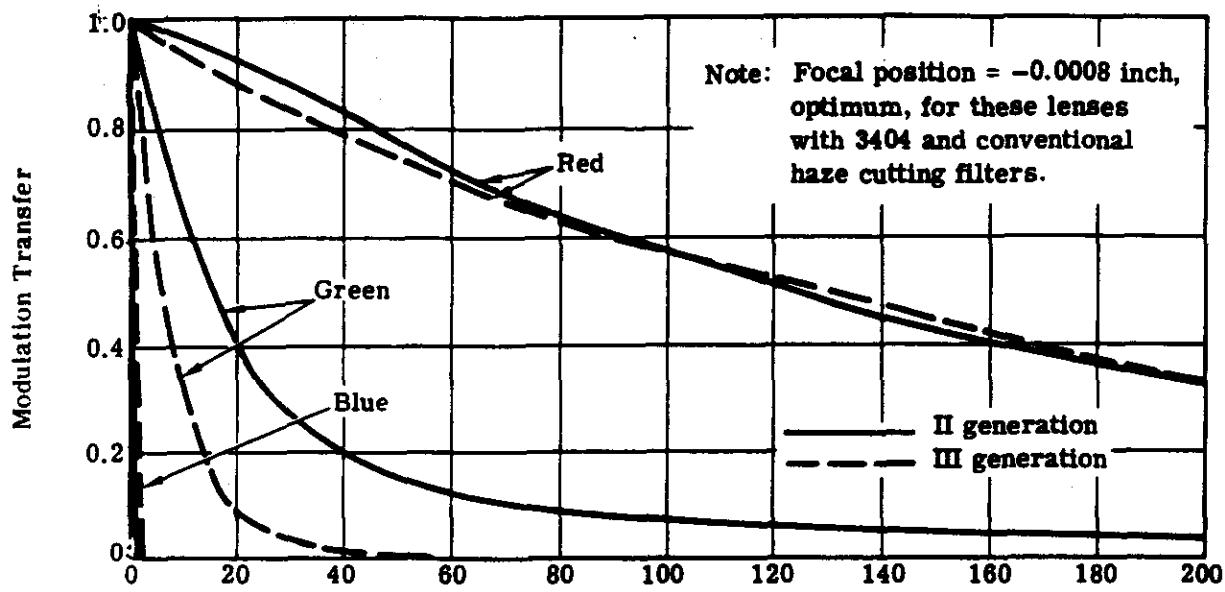

Fig. 4-1 — MTF's for second and third generation Petzval lenses for the three spectral sensitivities of SO-242 film

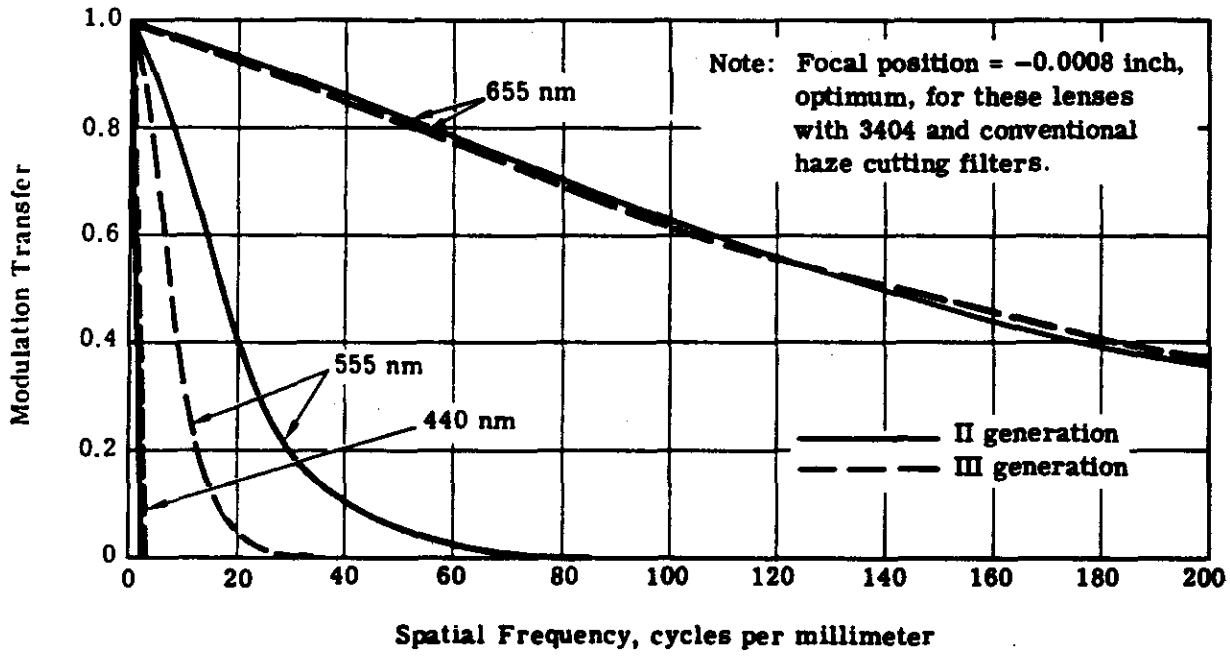

Fig. 4-2 — MTF's for second and third generation Petzval lenses for three wavelengths at the sensitivity peaks of SO-242 film

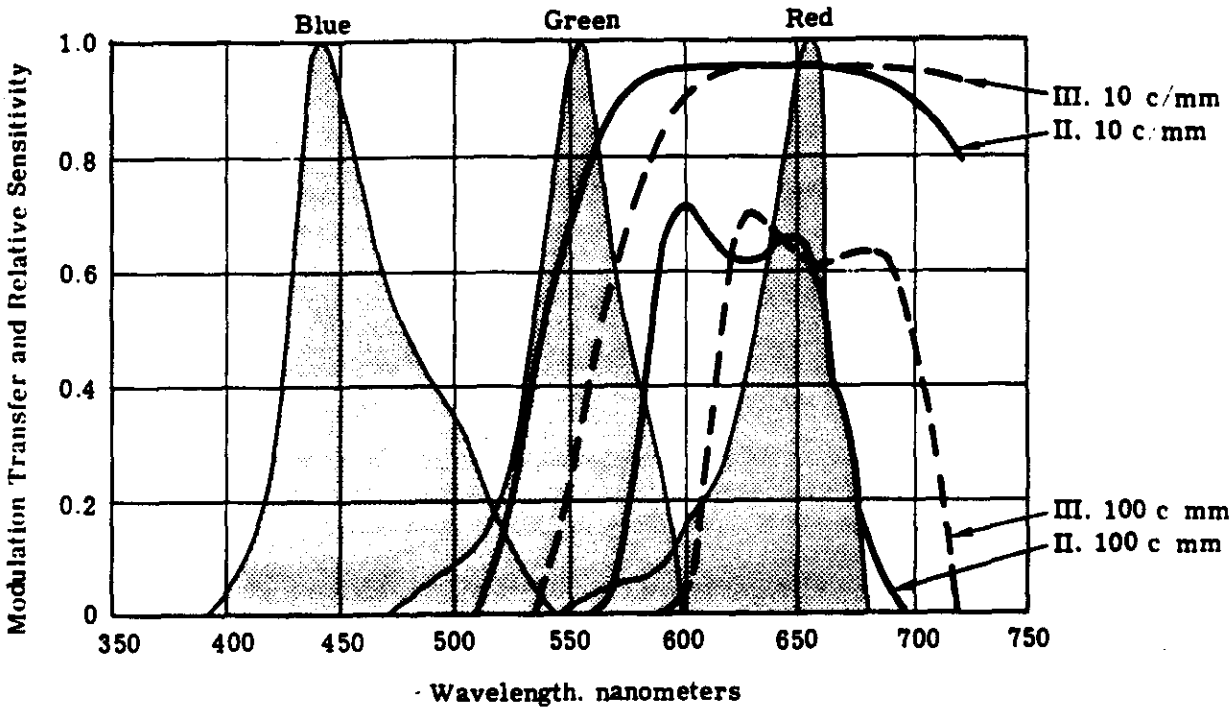

Fig. 4-3 — Comparison of Petzval lens modulation transfer contours

——— II generation
— — — III generation

Note: Modulation transfer for both second and third generation Petzval lenses was determined at best focus for 3404 with Wratten nos. 21 and 25, respectively.

separation due to the interlayer interaction of the dyes, as can be seen in Fig. 3-8. For example, when viewing or printing a color image with green light, most of the modulation is controlled by the magenta dye. However, there is some modulation being controlled by the yellow and cyan dyes as well.

In an ideal tri-pack color film, the dyes associated with the three layers would have spectral absorption distributions that were totally independent. In practice, however, this condition is never realized. A vector representation of the spectral density distributions of the dye layers can be used to determine a quantitative measure of the degree of independence of the layers. Values of the SO-242 normalized spectral density distribution (Fig. 3-8) of the individual dyes taken at 10-nanometer intervals were used as coefficients for unit vectors associated with the various wavelengths. For example, at λ = 510 nanometers, the spectral density coefficients are C = 0.16, M = 0.60, and Y = 0.27. The generalized equations are as follows:

$$\begin{aligned}
\vec{Y} &= y_1 \vec{\lambda}_{360} + y_2 \vec{\lambda}_{370} + y_3 \vec{\lambda}_{380} + \ldots + y_{45} \vec{\lambda}_{800} \\
\vec{M} &= m_1 \vec{\lambda}_{360} + m_2 \vec{\lambda}_{370} + m_3 \vec{\lambda}_{380} + \ldots + m_{45} \vec{\lambda}_{800} \\
\vec{C} &= c_1 \vec{\lambda}_{360} + c_2 \vec{\lambda}_{370} + c_3 \vec{\lambda}_{380} + \ldots + c_{45} \vec{\lambda}_{800}
\end{aligned} \tag{4.1}$$

where $\vec{C}$, $\vec{M}$, and $\vec{Y}$ refer to the cyan, magenta, and yellow dyes, respectively, and $\vec{\lambda}$ is the unit vector associated with the various wavelengths. This procedure was performed for the spectral region extending from 360 to 800 nanometers. Direction cosines were then calculated for the three possible dye-pair interactions:

$$\begin{aligned}
\text{Cos } (\theta)_{yc} &= \frac{\vec{Y} \cdot \vec{C}}{|\vec{Y}|\,|\vec{C}|} \\
\text{Cos } (\theta)_{mc} &= \frac{\vec{M} \cdot \vec{C}}{|\vec{M}|\,|\vec{C}|} \\
\text{Cos } (\theta)_{ym} &= \frac{\vec{Y} \cdot \vec{M}}{|\vec{Y}|\,|\vec{M}|}
\end{aligned} \tag{4.2}$$

where the numerators are vector dot products and the denominators are products of vector magnitudes.

The results for the SO-242 dye layer interactions are:

$$\begin{aligned}
\text{Cos } (\theta)_{yc} &= 0.2127 \\
\text{Cos } (\theta)_{mc} &= 0.3797 \\
\text{Cos } (\theta)_{ym} &= 0.3363
\end{aligned} \tag{4.3}$$

such that

$$\begin{aligned}
\theta_{yc} &= 77°41' \\
\theta_{mc} &= 67°41' \\
\theta_{ym} &= 71°25'
\end{aligned} \tag{4.4}$$

This technique gives a quantitative measure of the degree of dependence of the dye layers. Dyes that are totally independent would yield a direction cosine of zero (θ = 90 degrees), demonstrating orthogonality. At the other extreme, a direction cosine of unity (θ = 0 degrees) would represent total interaction or a repetition of the dye itself. In actual films, direction cosines are somewhere between these two hypothetical conditions. Eqs. 4.3 and 4.4 reveal that for SO-242 film the interaction between the yellow and cyan dyes is least severe, while the interaction between the magenta and cyan dyes is most severe. As can be observed in Fig. 3-8, the spectral density distributions of the yellow and magenta dyes tend to be narrow and localized, whereas the cyan dye is broad and spread out. Because of this encompassing cyan distribution, the cyan dye is involved in both the greatest and the least interactions.

4.3 INTEGRAL AND ANALYTICAL FILTER DENSITIES

When a microdensitometer is used with narrow band spectral filters to measure the red, green, and blue densities of a color film tri-pack, it effectively measures the major density contribution of the dye having maximum absorption to the spectral region being considered, but it also measures minor density contributions from the other two dye layers. These densities are known as integral filter densities (IFD's). The major contribution to the red, green, and blue densities (D_r, D_g, D_b) is from the cyan, magenta, and yellow dyes respectively. Therefore, making the assumption that the spectral density of the dye is proportional to the concentration of the dye (Beer's Law), the following equations can be written:

$$\begin{aligned} D_b &= A_{11}\,Y + A_{12}\,M + A_{13}\,C \\ D_g &= A_{21}\,Y + A_{22}\,M + A_{23}\,C \\ D_r &= A_{31}\,Y + A_{32}\,M + A_{33}\,C \end{aligned} \tag{4.5}$$

where A_{ij} is the coefficient for the density contributions of a particular dye to a particular "color" density, i.e., D_b, D_g, D_r.

These equations can be expressed as a matrix multiplication

$$\begin{bmatrix} D_b \\ D_g \\ D_r \end{bmatrix} = \begin{bmatrix} A_{11} & A_{12} & A_{13} \\ A_{21} & A_{22} & A_{23} \\ A_{31} & A_{32} & A_{33} \end{bmatrix} \cdot \begin{bmatrix} Y \\ M \\ C \end{bmatrix} \tag{4.6}$$

Therefore, in order to obtain the densities associated with the individual dye layers termed analytical filter densities (AFD's) and denoted here as Y, M, and C, it is necessary to take the inverse of the absorption coefficient matrix.

$$\begin{bmatrix} Y \\ M \\ C \end{bmatrix} = \begin{bmatrix} A_{11} & A_{12} & A_{13} \\ A_{21} & A_{22} & A_{23} \\ A_{31} & A_{32} & A_{33} \end{bmatrix}^{-1} \cdot \begin{bmatrix} D_b \\ D_g \\ D_r \end{bmatrix} \tag{4.7}$$

The absorption coefficient matrix $[A_{ij}]$ is determined by completely fogging two of the three dye layers and exposing a step tablet in the third dye layer. Red, green, and blue densities are then measured using the narrow band spectral filters previously mentioned to obtain the integral filter densities (IFD's). This results in three sensitometric curves for each dye layer, one for

the major density and one for each of the minor densities. Minor density values are then plotted against the major density values. Since a linear relationship exists over an extended range, the slopes (γ in Fig. 4-4) of the lines are taken as the normalized density coefficients. This procedure is repeated for each of the three dye layers. Since the major densities are plotted against themselves, their slope is unity, which results in an absorption coefficient matrix which has diagonal values of unity. Fig. 4-4 shows the minor densities plotted against major densities for each of the three dye layers as they were measured for SO-242 film. The absorption coefficient matrix for SO-242 film so determined was:

$$[A_{ij}] = \begin{bmatrix} A_{11} & A_{12} & A_{13} \\ A_{21} & A_{22} & A_{23} \\ A_{31} & A_{32} & A_{33} \end{bmatrix} = \begin{bmatrix} 1.000 & 0.066 & 0.023 \\ 0.172 & 1.000 & 0.043 \\ 0.069 & 0.069 & 1.000 \end{bmatrix} \tag{4.8}$$

This matrix was used in the determination of AFD's for all the work in the following sections.

4.4 SIGNAL AND NOISE PERTURBATIONS

In order to ensure that comparisons made between transfer functions for the three dye layers were representative, a neutral edge and step tablet made on a monochrome material were traced on the microdensitometer using the three narrow band spectral filters employed in the color work. The microdensitometer was refocused for each color. This is particularly necessary for the blue spectral region, since the achromat microscope objectives are not corrected for blue light. The transfer functions determined from these edge traces represent lens/film/microdensitometer combined transfer functions.

Since the lens/film transfer function used in making the test edge was not known, the microdensitometer MTF could not be determined directly. As an indirect estimation, the measured white light transfer function was converted to a previously accepted standard instrument MTF, and the conversion coefficients applied to the other "color" transfer functions as well (results are plotted in Fig. 4-5).

Transfer functions for the white, green, and blue regions are essentially the same. The marked deviation of the red transfer function, however, made it necessary to remove its influence from the Petzval lens/cyan dye layer transfer functions. The effect on the Petzval lens/cyan dye layer transfer function, although significant, is not large. For example, the difference between the corrected and uncorrected average Petzval lens/cyan layer MTF lies within the range of the data (Fig. 4-9). Although this experiment clearly shows a significantly lower instrument response in the red spectral region, it is the result of a single experiment and should be verified by measuring the instrument transfer function directly.

Transfer functions for the Petzval lens/SO-242 film layers indicate how the signal will be affected in the various dye layers. The quality of the image in a layer, however, cannot be described by transfer functions alone since the information available will be a function of the signal/noise interaction.

To illustrate the noise characteristics in each of the dye layers, red, green, and blue traces (176- by 1-micron slit) were made on SO-242 "neutral" density areas. The data was sampled at 1-micron intervals and converted to AFD's for plotting (see Fig. 4-6). Two different density levels were utilized in order to illustrate the noise characteristics at both high and low density levels. The yellow dye layer is much noisier than the other two dye layers, particularly at the high density. The effect of this high noise level will become evident in the following section.

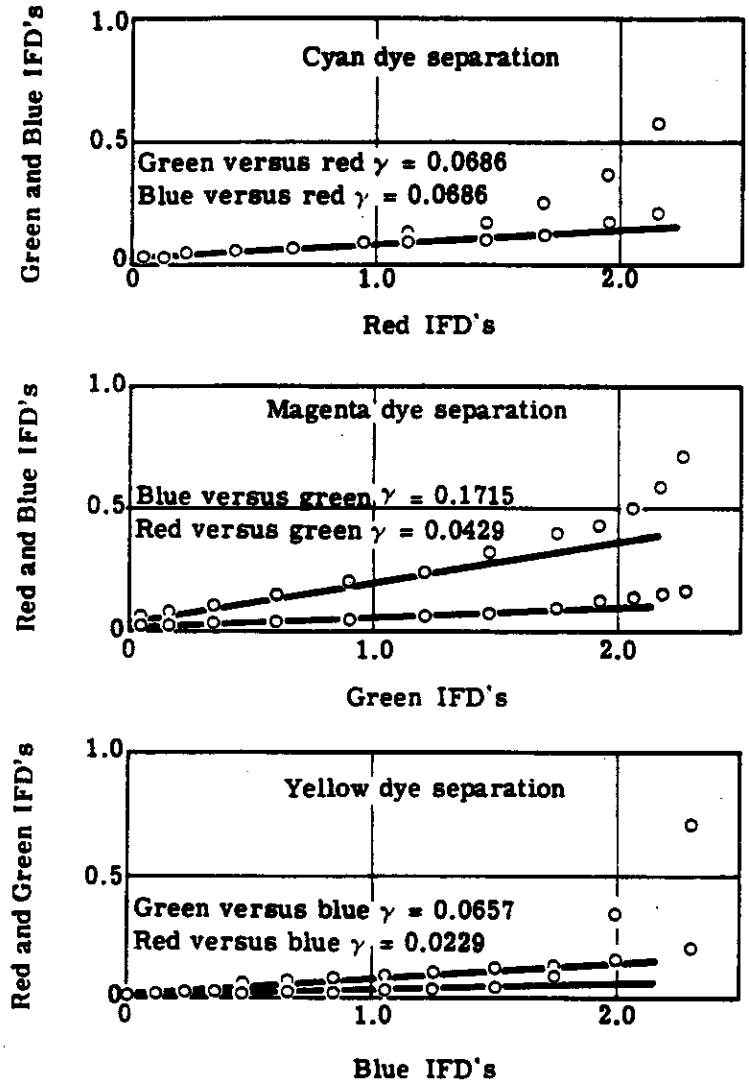

Fig. 4-4 — Minor/major density plots for SO-242 film

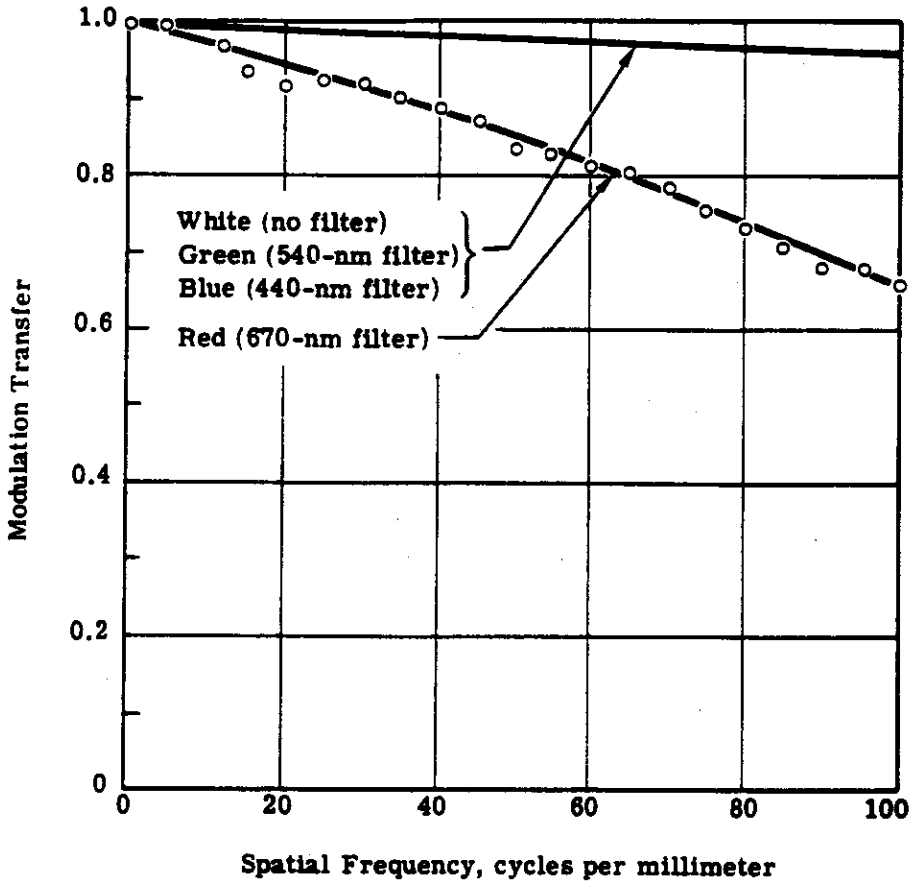

Fig. 4-5 — Microdensitometer MTF's for several spectral bands

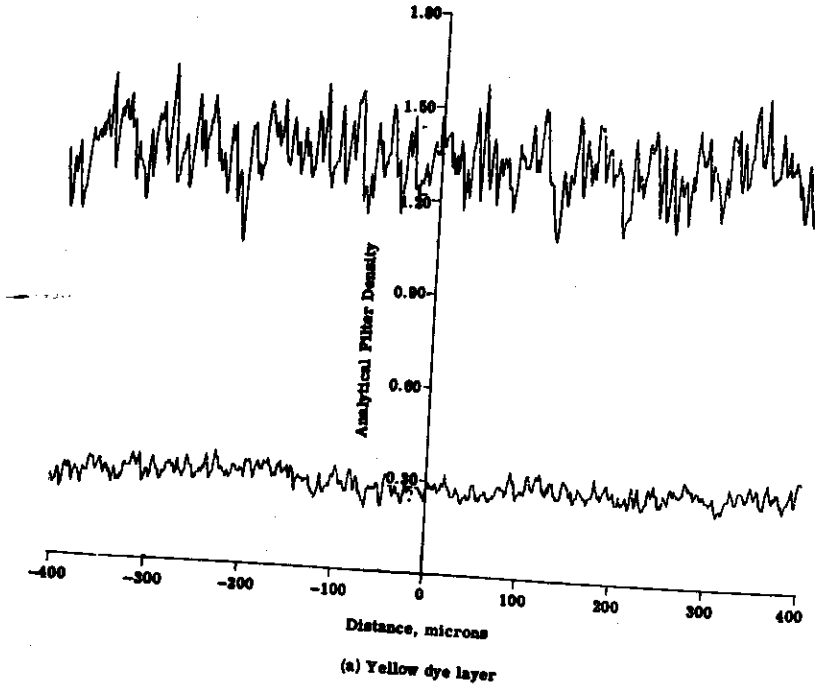

(a) Yellow dye layer

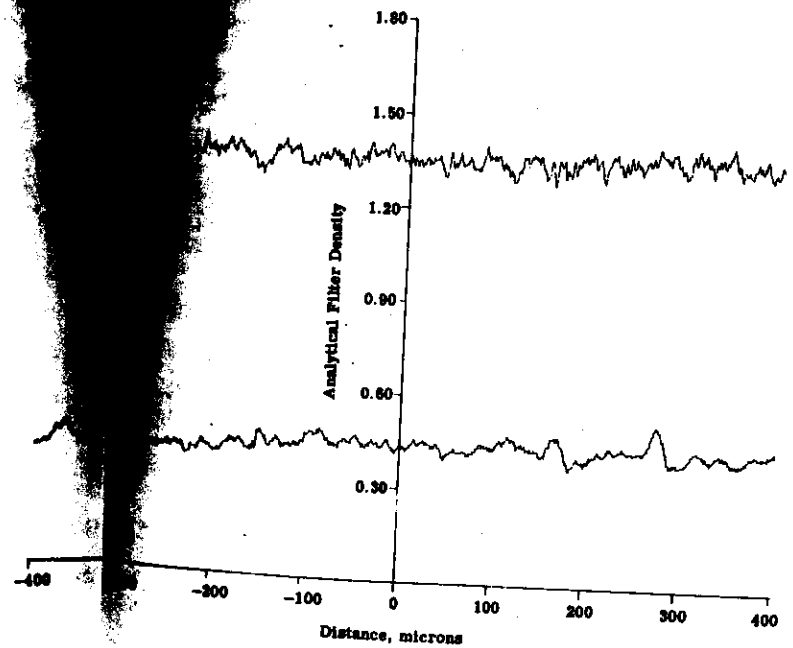

(b) Magenta dye layer

Fig. 4-6 — Photographic noise characterization in SO-242 film

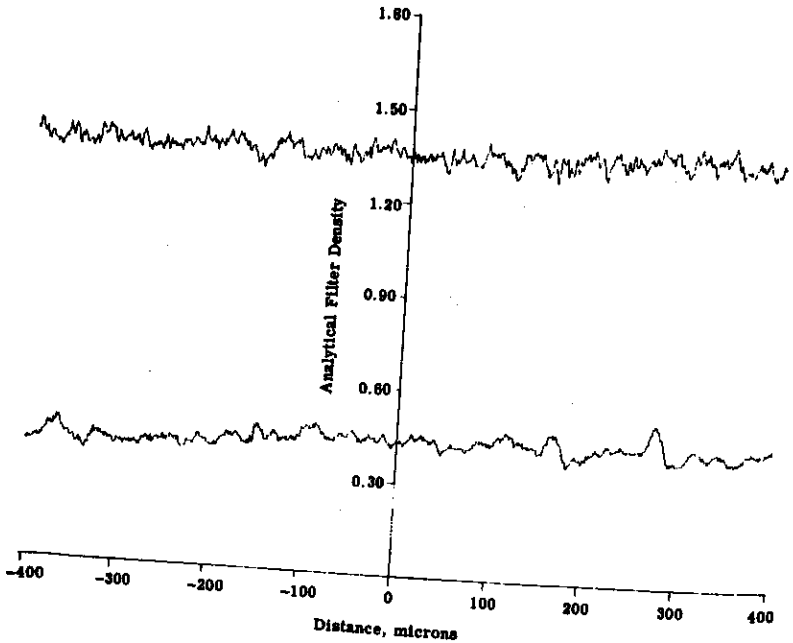

(b) Magenta dye layer

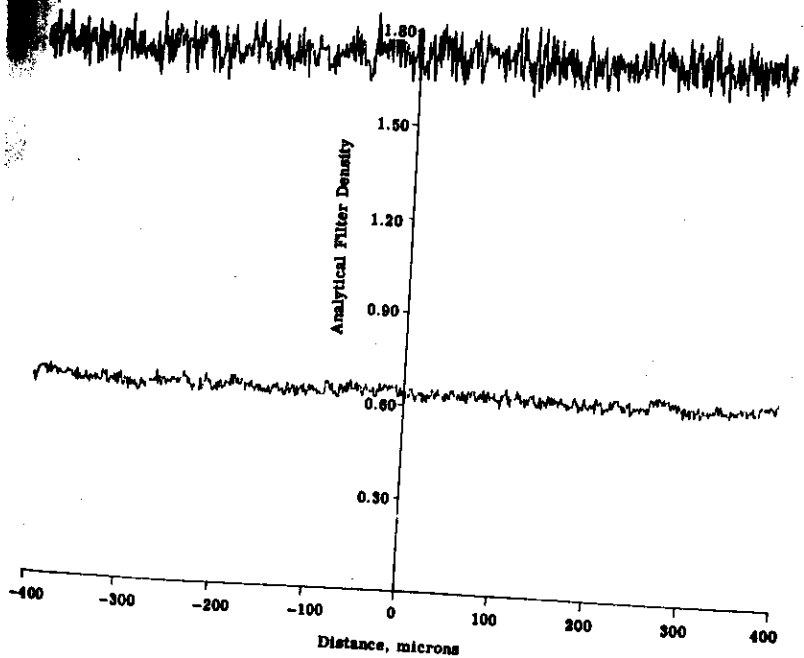

(c) Cyan dye layer

Fig. 4-6 — Photographic noise characterization in SO-242 film

The low frequency ripple present in the green and absent in the red was unexpected. However, scattering and shadowing caused by the silver halide particles in the magenta dye layer during exposure certainly affects the light distribution in the cyan dye layer. In addition, the measurements were made with the pelloid backing in place.

4.5 LENS/LAYER MTF DETERMINATIONS

In order to obtain an indication of the image quality capability of the KH-4B system with SO-242 film, transfer functions were determined from edge traces using imagery obtained with both second and third* generation lenses on the color film. Edges of photometric patches associated with imagery of low contrast (2:1) tri-bar targets were traced on the Mann microdensitometer with a 176- by 1-micron slit. The microdensitometer was equipped with three narrow band spectral filters having peak transmissions at 440, 540, and 670 nanometers in order to obtain IFD's for the SO-242 color film tri-pack. The appearance of an edge as viewed through narrow band spectral filters (IFD distributions) is illustrated in Fig. 4-7. IFD's were converted to AFD's (Section 4.3) and these values were converted to effective exposure using the sensitometry associated with the film strips. Once the effective exposure distribution of the edge had been determined, edge gradient analysis procedures† were employed. Fig. 4-8 shows a microdensitometer trace (IFD) of an edge, the analytical density distribution determined for the dye layer, its effective exposure distribution, and the transfer function determined for the lens/layer combination. In this particular illustration, the imagery was produced with a third generation lens and the distributions shown are for the cyan dye layer only. Analogous procedures were followed for all lens/layer combinations.

Composites of the replicate determinations of the lens/layer transfer functions for the cyan and magenta dye layers for both second and third generation lenses appear in Fig. 4-9. From these plots, the degree of experimental error in measuring these MTF's may be inferred. In Fig. 4-10 the IFD and AFD distributions are shown for the blue sensitive yellow dye layer. The transfer function is not presented, however, since the signal-to-noise ratio is so low even at spatial frequencies of 1 or 2 cycles per millimeter that a meaningful determination is not possible. The blue sensitive layer, being the bottom layer of the tri-pack, is also more susceptible to nonlinear effects such as adjacency. This complicates an accurate determination of the transfer function, since this nonlinearity is not removed by conventional sensitometry. Indications are, however, that there is a signal record in the blue sensitive layer, but its prime importance with this system is in terms of contributing to color balance and not to the resolution capability.

In Fig. 4-11, averages of the lens/layer transfer functions for the cyan and magenta dye layers are presented for both the second and third generation lenses. The important conclusion from this data is the fact that the lens/layer transfer function associated with the red sensitive cyan dye layer is limited by the film, whereas the green sensitive magenta dye layer is limited by the lens. This becomes apparent when the lens and lens/layer transfer functions are compared (see Figs. 4-1 and 4-11).

The fact that the green MTF's in both figures are essentially the same is associated with the out of focus condition of the magenta dye layer when the system is focused for red filtered

---

*Although the lens actually used to produce the imagery for this part of the work was a fourth generation (I-225) system, there is no discrepancy in making correlations with the calculations in Section 4.1.

†Blackman, Elliot S., Recovery of System Transfer Functions from Noisy Photographic Records, SPIE Image Information Recovery Seminar Proceedings, Philadelphia, Penn. (24-25 Oct 1968).

3404 film. The situation is depicted in Fig. 4-12 in which the focal positions of the peak sensitivity wavelengths are located on the optical axis of a second generation Petzval lens. Using geometric considerations only to simplify the point, it is clear that the size of the blur circles for the actinic radiation in each of the three sensitive layers are each different by an order of magnitude. Red light is focused in the magenta layer (at F_r), but this is only 0.0002 inch in front of the cyan layer such that the blur circle diameter is d_r = 2 microns. Green light is focused behind the film (at F_g) with the consequent blur circle diameter being d_g = 39 microns. Blue light is focused far down the optical axis (at F_b) creating a huge d_b = 555-micron blur circle diameter.

That the red MTF's are very much lower for the lens/layer combination (Fig. 4-11) than they are for the case of the lens alone (Fig. 4-1) is explained by a film MTF reduction in the cyan dye layer itself and the fact that light is incident on the red sensitive layer through a scattering medium, i.e., the green sensitive upper layer. It is therefore suspect to characterize image formation within integral layers using linear analysis since the scattering caused by the silver halide particles in the intervening layers is object dependent, that is, the scattering is dependent upon the light color and distribution and therefore its influence varies from point to point. The superiority of the second generation lens over the third generation lens suggested in Section 4.1 is now well defined by the lens/film transfer functions determined experimentally. Mission 1108 color imagery was acquired with a second generation lens.

For future tag-ons for which the system is focused for monolayer film, the performance level of the SO-242 color imagery with third or fourth generation lenses can not be expected to exceed that of the mission 1108 experiments. However, for a full load of color film in which the system is focused for an optimum tradeoff between the red and green layers, an improved performance is indicated.

(a) Magenta dye layer, Wratten no. 99 filter

(b) Cyan dye layer, Wratten no. 29 filter

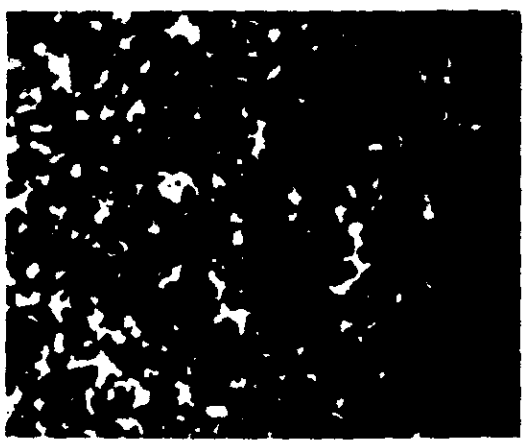

(c) Yellow dye layer. Wratten no. 47B

Fig. 4-7 — 450× enlargements of an edge imaged in SO-242 film reproduced through red, green, and blue filters

This page intentionally blank.

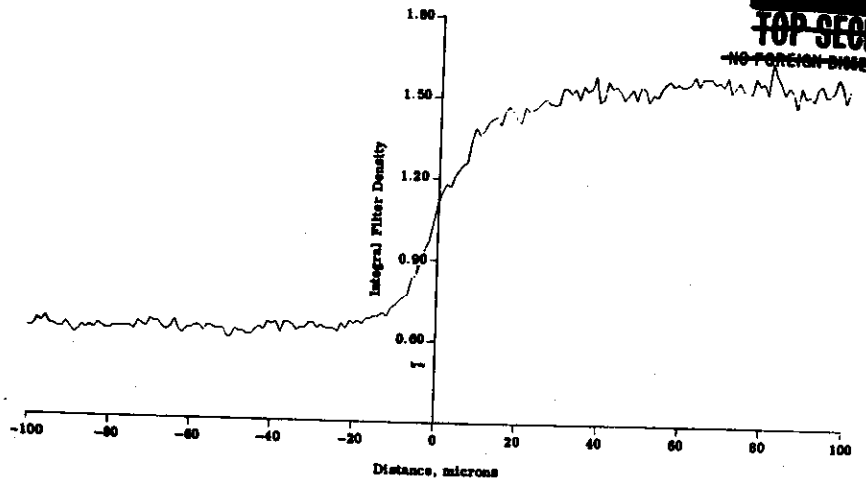

(a) Integral filter density

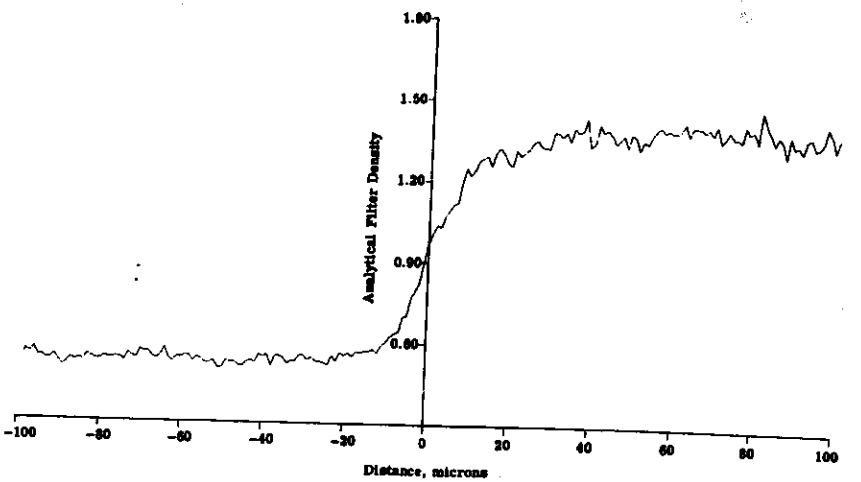

(b) Analytical filter density

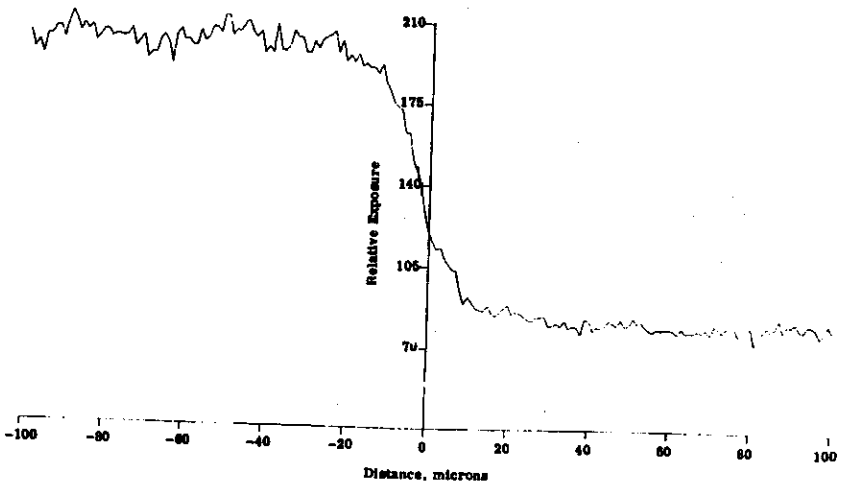

(c) Effective exposure

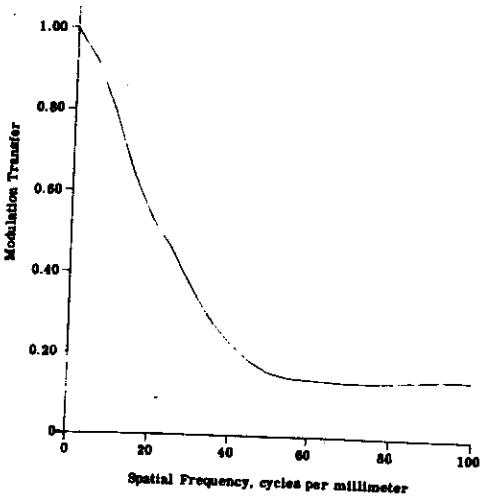

(d) Modulation transfer function

Fig. 4-8 — Illustration of steps involved in producing an MTF from a single edge trace for the cyan dye layer of SO-242 film imaged with a third generation Petzval lens

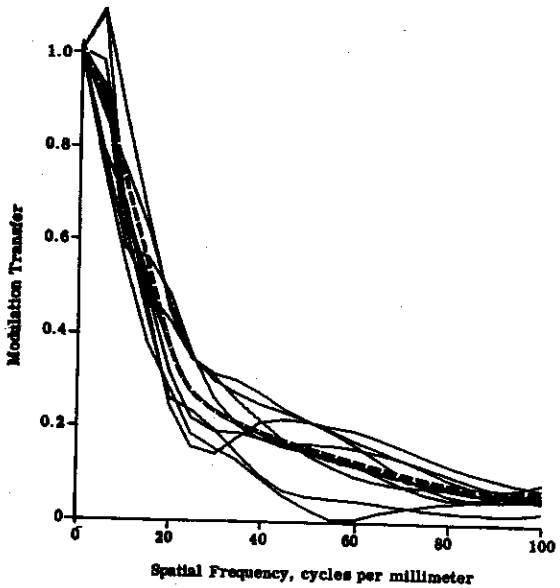

(a) Second generation Petzval/SO-242 magenta dye layer

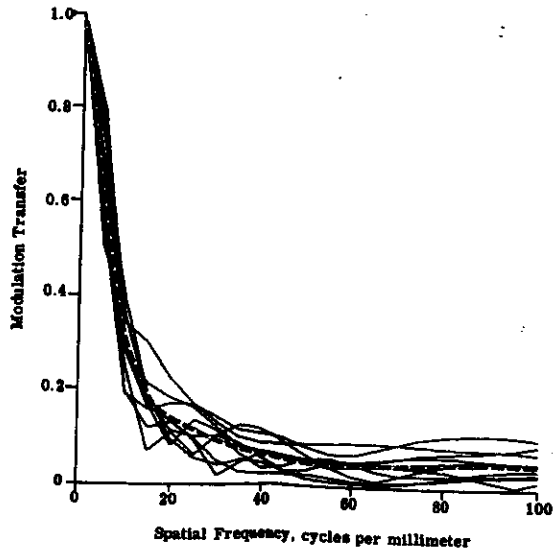

(b) Third generation Petzval/SO-242 magenta dye layer

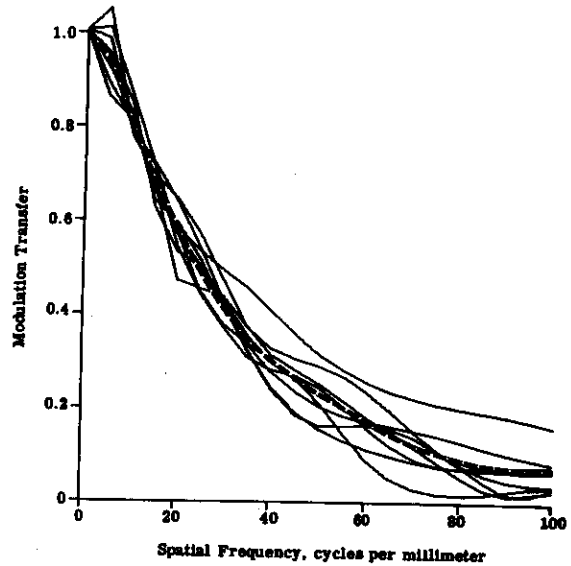

(c) Second generation Petzval/SO-242 cyan dye layer

Fig. 4-9 — Lens/film MTF's determined from edge traces

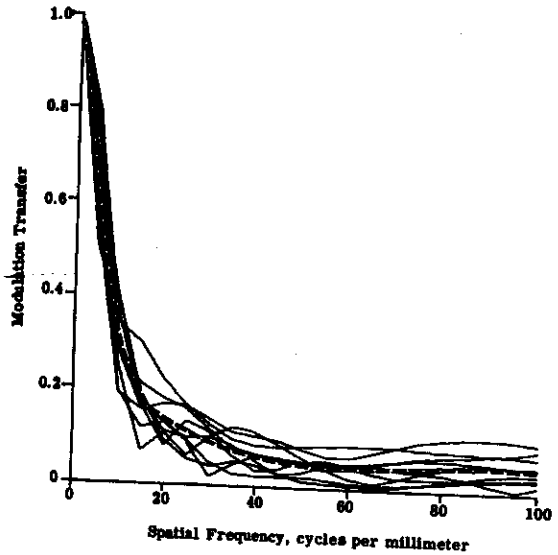

(b) Third generation Petzval/SO-242 magenta dye layer

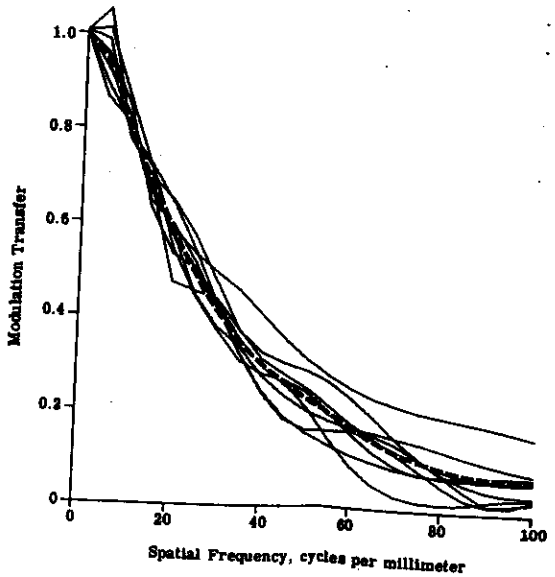

(c) Second generation Petzval/SO-242 cyan dye layer

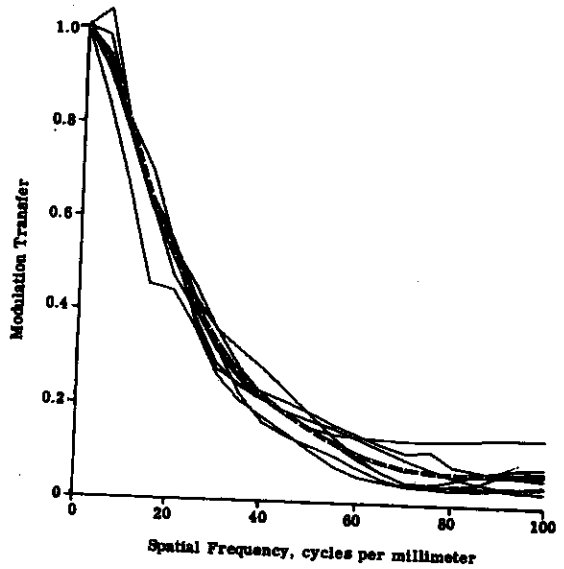

(d) Third generation Petzval/SO-242 cyan dye layer

Fig. 4-9 — Lens/film MTF's determined from edge traces

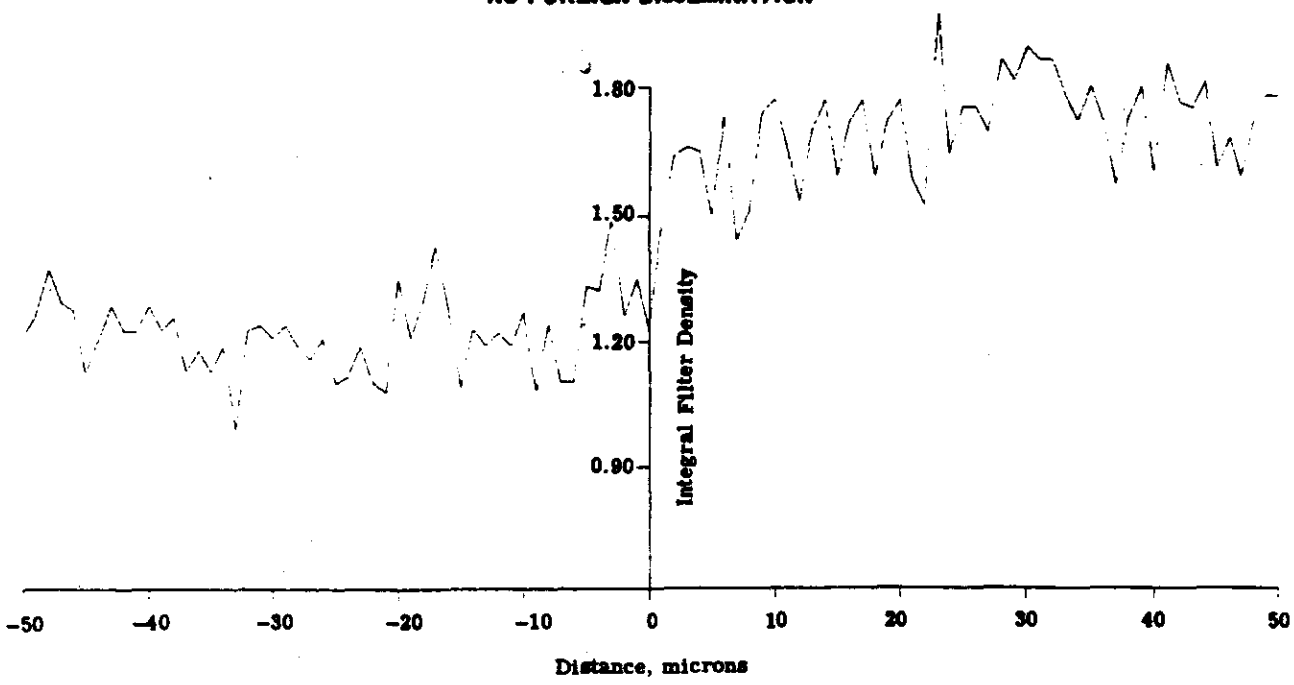

(a) IFD

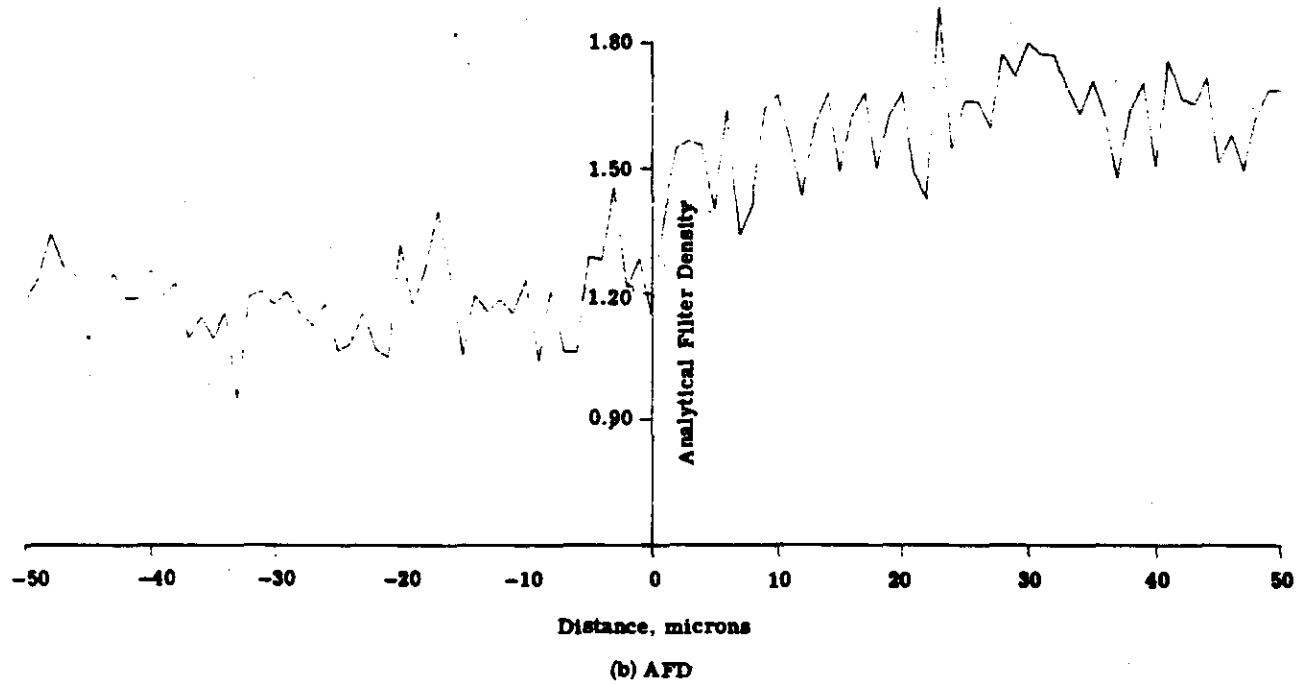

(b) AFD

Fig. 4-10 — Yellow dye layer IFD and AFD edge distributions

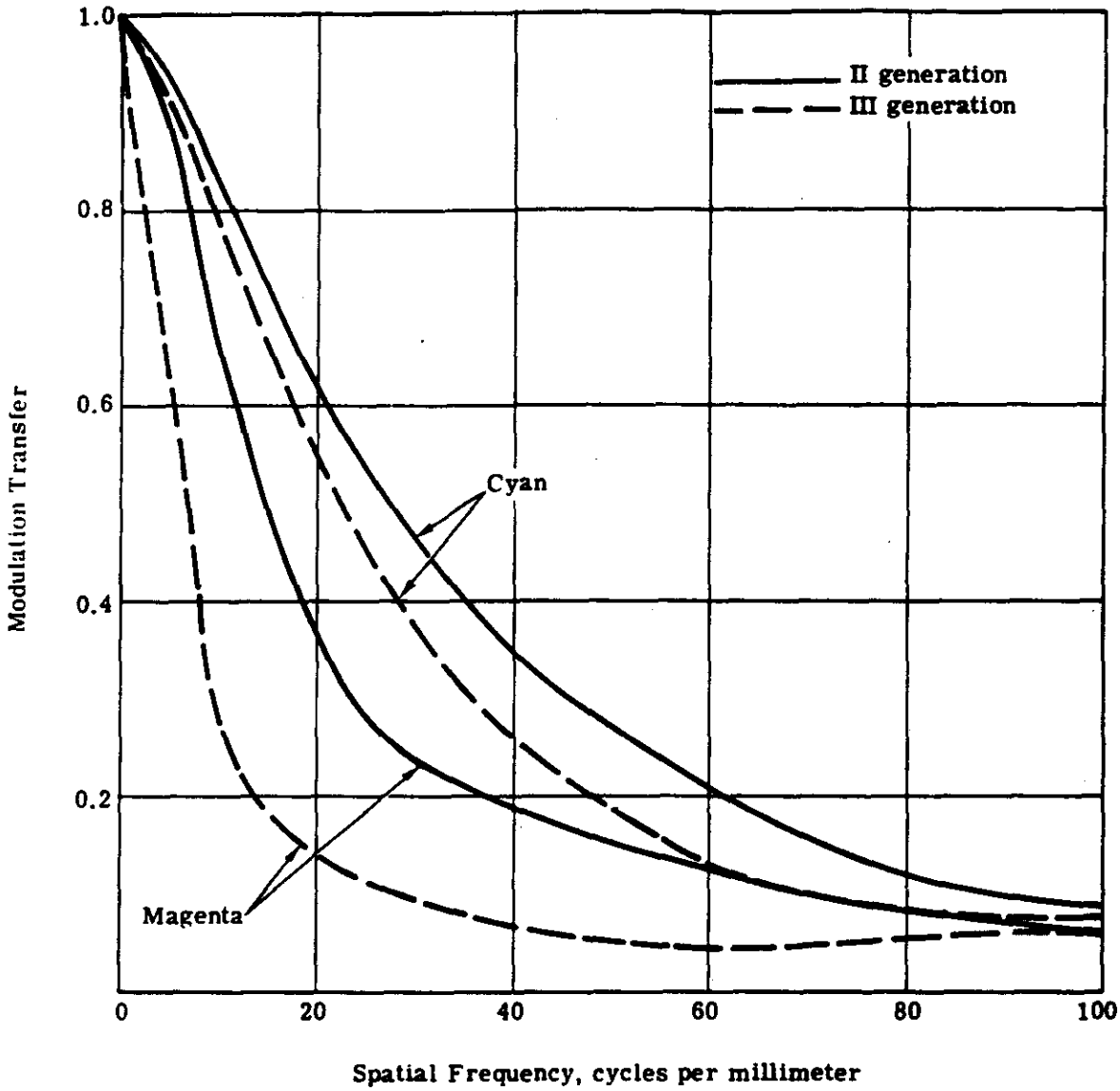

Fig. 4-11 — Average Petzval lens/SO-242 dye layer MTF's determined from edge traces

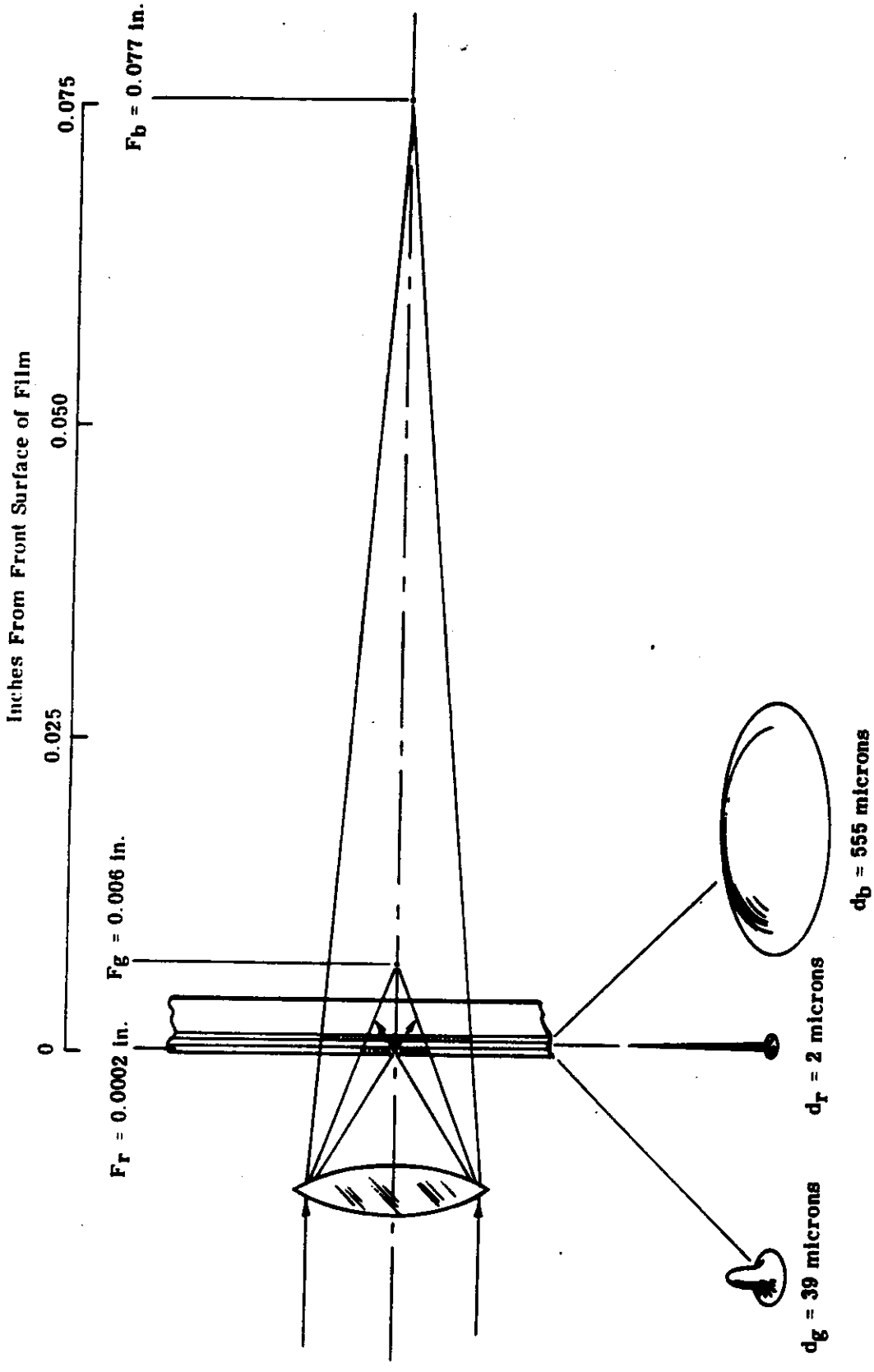

Fig. 4-12 — Illustration (not to scale) of relative size of blur circles for the actinic radiation in each of the SO-242 film layers

This page intentionally blank.

5. INTERPRETABILITY OF MISSION 1108 SO-242 IMAGERY

Color film has the unique capability of imaging the world "as it is" with the hue and saturation added to the neutral tone patterns recorded in black and white film. Previously, SO-121 film performed well insofar as it showed that natural color coverage could be successfully acquired by the KH-4B cameras. Before that, SO-180 film had been used with limited success.

In order to evaluate the interpretability of the mission 1108 SO-242 imagery, an intensive subjective study was carried out. Results of this photointerpretation work are set forth in the following sections. Adjunct to the text are photographic enlargements made from the mission imagery, designed to illustrate many of the principal observations. Judgmental comments are quantified in terms of a psychometric ranking system developed for this program and utilized similarly in the KH-4B SO-121 and SO-180 Capability Reports. The psychometric ranking system is described in Appendix A. Interpretability was explored in an all-inclusive mode, and is presented in an ordered way by developing seven different subject areas independently. These subject areas include targetry and context associated with culture, military, vegetation, cultivation, hydrology, atmosphere, and geology. Relative subjective evaluation matrices for the SO-242 for clear coverage and snow coverage are given in Fig. 5-9. For comparison, the matrices from the SO-121 and SO-180 experiments are given in Fig. 5-10.

5.1 RESOLUTION EVALUATION

Improved resolution claimed for SO-242 versus SO-121 is indeed apparent. This new color film is noticeably better in recording fine detail and rendering edge acuity than both the SO-180 and SO-121 media. This is well exemplified with targetry such as small buildings, for example.

A measure of resolution at the film plane and its corresponding distance resolved on the ground was made using an indirect method, since no resolution targets were acquired during the color passes. The technique involved searching the black and white record and the color record simultaneously for man-made objects that somewhat resemble resolution targets, i.e., equally spaced light and dark linear objects. In selecting an appropriate target, the imagery of the color record must be at the limit of resolution. A medium contrast film resolution target is then placed over the black and white image and a match of spacing is made with the three-bar elements. This gives the film resolution in cycles per millimeter at the SO-242 threshold of resolution. With this figure established, the operational parameters are extracted from the mission ephemeris, and the ground resolved distance is calculated.

Suitable imagery was found in rev D-252, 002 forward (x = 69.1, y = 1.7),* 008 aft (x = 5.6, y = 4.5)* about 30 degrees off the center of format. A resolution level of 58 cycles per millimeter for SO-242 was derived from this imagery. No usable configuration was found any closer

*Universal grid coordinates.

to the center of format. Image scale in the scan direction was calculated to be 1:430,400 by using the formula

$$\text{Scan scale} = \frac{H}{(F)(\cos\phi)(\cos^2\theta)}$$

where H = vehicle altitude, feet
F = focal length, feet
ϕ = camera convergence angle (15 degrees)
θ = scan angle, degrees

Reduction of film resolution to ground resolved distance is accomplished by using the formula

$$GRD = \frac{S}{(304.8)(R)}$$

where GRD = ground resolved distance, feet
S = scale of image
R = resolution of film. cycles per millimeter

A GRD of 21 feet for the scan component was calculated.

A second area of limited use for resolution determination was found in rev D-264, 008 forward and 014 aft. Two frequency patterns were measured. That which measured 57 cycles per millimeter on the 3404 was not resolved on SO-242. That which measured 40 cycles per millimeter was well resolved. The average of the two is 49 cycles per millimeter, well matched with the previously calculated figure.

Since the resolution capability was determined from a second generation duplicate, it is reasonable to assume about a 20 percent increase in this frequency range based on past experience. The original camera material covering the items measured was not available for examination. Performance level of the original taking material is therefore estimated to be 60 to 70 cycles per millimeter, corresponding to a 15-foot GRD level.

Comparison of original and duplicate records of other passes of the color test revealed a bonus obtained for some items by the reproduction process. Contrast is increased by duping, and several cases were observed in which fine detail was accentuated and, in effect, the apparent resolution increased. This was particularly true for items of low reflectance against a somewhat similar background.

For comparison, the calculated resolution capabilities of four KH-4B mission color experiments are listed below. These values are derived from duplicates, so adjustments must be made for losses occurring in the reproduction process.

Mission	1104	1105	1106	1108
Color film	SO-180	SO-121	SO-121	SO-242
Direction	IMC	SCN	SCN	SCN
Film resolution, cycles per millimeter	24	45	32	58
Ground resolved distance, feet	36	24	27	21

5.2 COLOR EVALUATION

Snow, which recorded as slightly blue or cyan on the original, was rendered quite neutral on most of the duplicates. Comparing the neutral discs at the beginning of each roll, it was noted that those on the duplicates showed a decided magenta cast, corroborating the observation.

Operational use of SO-242 in December induced a limiting factor into the evaluation; much of the coverage is snow-covered terrain. In general this produces a quasi-monochromatic record with white snow and greenish-gray detail (Fig. 5-2). Coupled with the lower resolution and higher graininess, the results are far inferior to the 3404 results (Fig. 5-1). In some isolated instances a color signature will appear in the form of a distinctive smoke plume or some similar item, but these are few in number.

Because of the distinct differences between those passes having snow cover and those that are clear, two separate subjective evaluations were made (Fig. 5-9). Note that exposure for these two illumination conditions was estimated independently with "snow" and "no snow" EV curves (see Appendix B). Five passes had snow cover and eight had bare ground.

Cloud cover, haze, and low solar elevations degraded a number of passes in the test, even to the point of elimination from consideration. Most of the color photography, however, was amenable to evaluation. The color experiment involved 13 revs commencing with D-242 and finishing with D-274. Three revs included parts of the United States, one of them extending into Cuba, and 10 covered Eurasia. The specific locations of these acquisitions are given in Figs. 2-1 and 2-2.

Stereo viewing of the film records affords a point by point comparison of the merits or deficiencies of either record. At the same time the stereo model permits the viewer to observe in three-dimensional color and relate more completely to the area. Using color and black and white simultaneously produces a stereo condition in which the color of SO-242 complements the high resolution of 3404. Differences in the image brightness (in viewing the film transparencies) may cause one eye or the other to assume dominance. This can be controlled quite simply by inserting a neutral density filter in the 3404 channel. A comfortable balance is acquired by trial. A 0.9 ND proved adequate for this evaluation.

As an aid to presentation of the subjective evaluation results and as a standardized reference frame, the comparisons contained in this report have been assigned values (see Appendix A). This is the same reference used for the SO-180 and SO-121 Capability Reports, and the results of these investigations have been included (Fig. 5-10) for comparison.

5.3 SPECIFIC SUBJECT EVALUATION

5.3.1 Culture

Intelligence, for the most part, deals with the works of man—his cities, transportation networks, industry, and military facilities. Resolution limitation of the color record is apparent in the recording of cultural objects. Small items of a nonextended nature are generally rated poor (rank 3) to fair (rank 4). Individual dwellings may be accurately counted in the color record if there is sufficient contrast with the background. Low reflectance roofs tend to become lost. Geometry of small structures and separation from adjoining objects and background are severely limited by the lesser resolution of SO-242 (Figs. 5-1 through 5-6). The assigned ranks apply in both clear and snow cases.

As size of the buildings increases, detection and overall delineation improve to fair (rank 4) and good (rank 5). Naturally, small components and appendages do not show on the color film. Color signatures do play a role in identification, as has been cited in previous reports. Copper waste slurry (Fig. 5-6) is readily identifiable by color though the resolution is better on 3404 (Fig. 5-5). In this instance the massive size of the object precludes any real need for detail. The color identification capability of SO-242 is superior (rank 8) in this sort of facility.

Various transportation networks are affected by the absence or presence of snow cover. Roads through residential areas tend to lose their identity because of a lack of contrast. Alignment is often indicated by the orientation of buildings or trees (Fig. 5-2). Traffic over these same roads after a snowfall will change the color by melting or soiling and form an easily visible contrast with the undisturbed snow. Transportation routes through areas with snow cover rank from fair (rank 4) to equal to 3404 (rank 6), depending on local conditions. For those areas clear of snow, ranking is predominantly fair (rank 4) to good (rank 5) with an occasional sample equal to 3404 (rank 6).

Railroads are recognized on the SO-242 primarily by their alignment and layout characteristics and are fair (rank 4) by comparison with the standard film (Figs. 5-1 and 5-2). Detection of vehicles on railroads (or highways) is not possible (rank 1) with color, but the occasional plume of smoke from a locomotive may show its presence indirectly.

Airfield detection, location, and delineation with the color film is equal (rank 6) to the standard 3404. As the objects to be interpreted decrease in size, the ranking also decreases (Fig. 5-7). Facilities are good (rank 5); aircraft count is good (rank 5) for large aircraft, fair (rank 4) for small; and aircraft identification is at the threshold of interpretability (rank 2).

Generally, it may be concluded that the relative interpretability ranking number increases with the size of the subject to a level of about fair (rank 4) to good (rank 5). Resolution is the limiting factor as might be expected. Only those items having a large size and/or a distinctive color signature, such as airfields or copper refineries, rank equally (rank 6) or higher than the standard 3404 film.

5.3.2 Military

Military installations approximate cultural developments in most respects. They consist of buildings, built-up areas, roads, airfields, vehicles, etc. The major difference lies in their use and distribution. Military installations need not be located in an area offering economic or aesthetic incentives as a civilian population center usually does. They are distributed to provide the best support function or the most advantageous defensive or offensive posture. Thus, military facilities are often remotely or unusually situated.

The passes evaluated provide a sampling of some representative facilities. Most of the military airfields found were only fair (rank 4) compared with the 3404, and two ranks below the larger civilian facilities covered in this mission. The exception was Davis Monthan AFB in Arizona (Fig. 5-7). Strike aircraft such as the B-52 were easily recognized, but structural details that would indicate the model are missing. Comparison is made with a similar facility recorded on SO-121 from mission 1105. The SO-121 allows a count of aircraft and a probable determination of type. SO-242 permits identification, but both color films fall short of 3404 in specific information content.

Defensive missile launch sites and rocket test facilities are snow-covered in the mission photography and are fair (rank 4) by comparison with 3404. While fine detail is lacking in the color record, the perspective provided by the panoramic coverage together with the shadow

outlines provided by the look angle present useful interpretation clues. The configuration of the facility is accentuated, and related facilities are delineated better by the fact that the shadow is falling on snow and provides higher contrast than if it fell on natural ground. The layout of a launch complex and the size of a large radar structure are apparent in Fig. 5-2. Subtle relief is also well rendered in snow-covered imagery, as illustrated in Figs. 5-1 and 5-2. These vertical differences may or may not be measurable with mensuration instruments, but they are visually detectable due to the enhancement from the smooth ground cover of snow and the low solar angle.

Communication antennas are usually composed of parts below the level of detectability as defined by three-bar targets. Elongated lines, though, have a much higher detection threshold. This was readily apparent in the ability to detect a circular antenna configuration and define its shape and limits on the SO-242 even though the individual structural members are very narrow, much smaller than the 15-foot GRD level. The length of the components and the snow background were the main contributors to its being observed.

5.3.3 Vegetation

Vegetation occurring naturally in the areas covered by SO-242 are better (rank 7) to superior (rank 8) for the clear ground imagery and good (rank 5) for snow cover when related to 3404. Delineation of the limits of stands of trees is about the same, since this is well within the resolution capability of both films (Figs. 5-1 and 5-2).

Texture and separation of timber and scrub as well as many other distinctions are hampered by the use of a Wratten no. 25 filter. The cutoff frequency is 600 nanometers, beyond the peak reflectance area of green vegetation in the visible portion of the spectrum. This will produce the dark, featureless expanses of trees seen in some of the passes, particularly those with wooded mountains. Desert vegetation was covered extensively in rev D-242. Many of the higher elevations were created by volcanic activity and appear as very dark on the 3404. SO-242, however, shows this darkness is not a rock tone but rather a vegetative cover which appears dark on the 3404 record. Alluvium at the out-fall of erosional gullies also show the profusion of growth due to the amount of water present in these features. Trees and scrub growing along the washes are detectable to an equal amount (rank 6) in both records, but sand deposits at bends tend to promote growth that is better distinguished on the SO-242.

5.3.4 Cultivation

Cultivation is treated as a separate subject apart from vegetation because of the conscious and orderly methodology employed and the vital importance of food to the strategic posture of a nation. The time period covered by this mission is in December, not a particularly good growing season in the northern latitudes. Those passes having a snow ground cover naturally can contribute no information regarding crops except for delineation of plots and fields. Areas with no snow show color differences in fields. These are primarily the normal dying-off colors of harvested fields or pasturage.

Atmospheric conditions, mostly haze, reduce the contrast of the Chinese agricultural areas in rev D-248, but the types of crops are distinguished equally well (rank 6) on the SO-242 and 3404. Extent of cultivation is superior (rank 8) for color in spite of the degrading atmospheric conditions. Except for special purpose use, color photography of agricultural areas should be limited to those seasons when meaningful activity is in progress.

5.3.5 Hydrology

Hydrologic interpretation is dependent on many factors, some which apply in most cases and some which apply in only special instances. Drainage through arid areas may be merely a slight depression of narrow cross section. Though these depressions may fall below the resolution threshold of SO-242, their length often makes them detectable but only fair (rank 4) compared with 3404. A mantel of snow often obscures some detail reducing the evaluation to poor. Though the leveling effect of the snow is apparent, a low sun angle often accentuates the dips as mentioned in reference to suble relief in Section 5.4.2.

The stimulation of vegetative growth along water courses, even for subsurface flow, provides a secondary key to drainage. Depending on the configuration and other associated factors, the SO-242 is from fair (rank 4) to better (rank 7) than 3404.

Defining the limits of seasonal flooding and determining the presence and extent of ice and snow are better (rank 7) for the color film. Color signatures for these items render them more distinguishable than the neutral tones of black and white photography. The original color material shows the snow cover as more blue-cyan making it difficult to separate snow, ice, and rocks. The duplicate color material renders such situations more in their natural colors and therefore easier to interpret.

The duping process, in addition to rendering a more neutral image, accentuates most features by additional contrast and higher saturation. In clear water there are two methods of depth determination. Stereo viewing with high resolution black and white film utilizes the bottom and surface detail and those items awash, such as rocks and reefs. This first method generally ranks higher than color, SO-242 being fair (rank 4) by comparison. A second method uses the spectral absorption characteristics of water and the reflectivity of the bottom. The duplicate color print exhibits more blue than the original camera material. The color shifts must be considered if analysis by the second method is applied.

Sunlight passing through water loses color as a function of depth. Infrared radiation is absorbed within inches of the surface. Red wavelengths are found to a depth of about 20 feet in clear water, orange to about 25 feet, yellow to about 35 feet, and green extends to about 100 feet. Beyond this depth there is only blue light until totally attenuated by the mass of the water column. Of course these attentuations are dependent on the clarity of the water and the presence of dissolved substances or plankton which might color or filter the light. Table 5-1 is an illustration of differences measured in various sea locations and underscores the variability of conditions for which compensation must be made.

When observed from directly above the surface, the illuminating source must travel a double path through the water. Thus, loss of any given wavelength by absorption will be at half the depths mentioned above. Fig. 5-8 illustrates only the case for SO-242 because no 3404 coverage of the area was obtained (camera shut down). Loss of spectral information is also affected by the look angle, the more oblique having a longer path through the water. In addition, light incident on the surface becomes more diffuse with depth, the more vertical coverage having a more specular component. Regardless of the degrading factors though, orbital color records may range as high as superior (rank 8) or exceptional (rank 9) compared with the 3404 panchromatic record.

5.3.6 Atmosphere

Atmospheric assessment could be classified in two ways: (1) how well are airborne signatures depicted; and (2) how do airborne particles obscure the ground imagery? In the first instance, the

Table 5-1 — Comparison of Percentage Absorption of Light Per Meter for Unfiltered Samples of Sea Water From All Stations Measured After Shaking*

Curve	Locality
1	Sargasso Sea
2	Continental Slope
3	Continental Shelf
4	Vineyard Sound Whistle Buoy
5	Vineyard Sound
6	Buzzards Bay

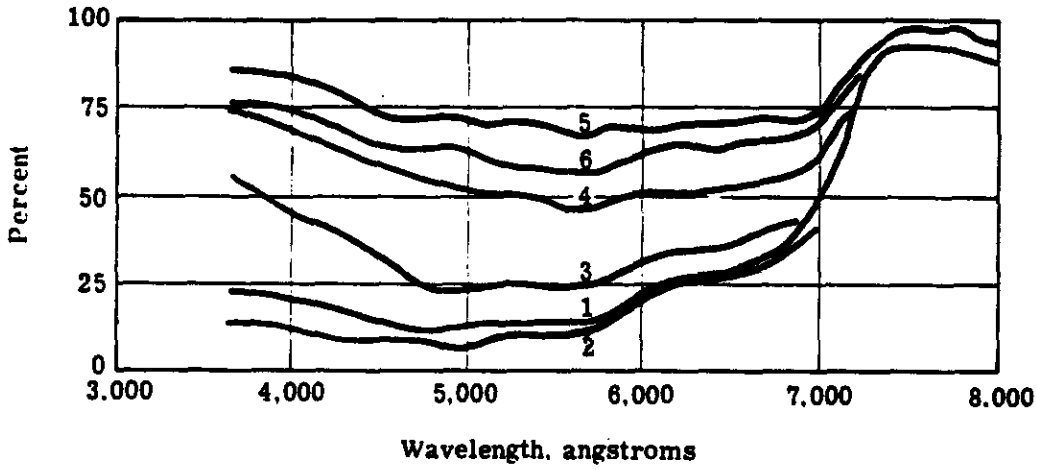

*Clarke, G. L., and James, H. R., J. Opt. Soc. Am., Vol. 29, p. 52, 1939.

presence of smoke without a characteristic color is less obvious on SO-242 and ranges from a low of poor (rank 3) through good (rank 5) to equal (rank 6). The higher values are more commonly found in the snow coverage where the background is nearly equal for comparison. Where the color of the ground features form a backing for the atmospheric particles, their effect shows less distinctly in the color.

Penetration of the intervening air column is about equal (rank 6) for both the SO-242 color and minus-blue filtered panchromatic 3404. In one case hue differences provide the apparent visibility, and in the other the haze penetration by filtration accentuates the differences.

5.3.7 Geology

As in previous studies using color films, the geologic characteristics of the areas covered by the mission are unusually well presented. The synoptic view afforded by the system being orbital, panoramic, and stereoscopic is exceptional. Structural entities are encompassed and fine details are faithfully recorded. The use of a color record in conjunction with a panchromatic record provided a vast increase in information content for those skilled in geologic interpretation. Those passes with snow cover are equally (rank 6) well shown on both films. Much of the color related information is obscured. Only a thin mantle is required to eliminate most hue distinctions. General configurations are still present, though, and the structural information contributed by the drainage is still visible.

Those parts of the color mission coverage which are free from snow, and particularly those areas free of clouds and vegetation, are either superior (rank 8) or exceptional (rank 9) compared to 3404. Stratification is well delineated in black and white. SO-242 provides a hue signature that aids in identification and sequence determination. Figs. 6-5, 6-7, and 6-8 have examples of this feature. Parent rock to soil differences are evident and the distribution and stratification of alluvium, particularly where incised by drainage (Figs. 6-3 and 6-4) are judged superior (rank 8) and exceptional (rank 9). Various low areas are the locations of ponds that are in actuality evaporation beds. Salts and alluvia are deposited here by runoff, and the subsequent loss of water by evaporation concentrates and stratifies, thus producing vivid colored areas (Figs. 6-3 and 6-4).

The interpretation of geology does not require high resolution. That which is obtained with SO-242 in this system is more than adequate for initial reconnaissance and delineation. Enlargement of selected areas to appropriate scales allows a more detailed examination.

Stereo is almost indispensable. The structure of the area within the stereo model is vividly apparent and determination of strike, dip, relative height differences, and texture on a subjective level is greatly enhanced (Fig. 6-6). Combined with color, the presentation to a trained observer is unparalleled. A professional geologic assessment of a sample of the SO-242 imagery is presented separately in Section 6.

5.3.8 Summary

That the KH-4B camera system is able to use color film (SO-121) and produce usable imagery was adequately demonstrated by missions 1105 and 1106. Mission 1108 (SO-242) has now amplified the conclusions reached in these experiments. This amplification is made possible by increased resolution capability and better color contrast. Reference to the relative subjective evaluation matrices (Figs. 5-9 and 5-10) shows that there is a general across-the-board increase in the rankings with later missions. Thus, the information content increases as one proceeds from SO-180 through SO-121 to SO-242. In making these comparisons, however, the information content loss due to snow cover must be taken into account.

Those categories ranking lower are those whose interpretation is dependent more on resolution than color, i.e., culture, military, and transportation. The "natural" categories of geology, hydrology, cultivation, and vegetation all rank higher. These are areas of interest where color and shape are the more important considerations. This overall polarity is generally true for all three color films (SO-242, SO-121, and SO-180) in the KH-4B system.

The routine intelligence questions addressed to KH-4B coverage were much better answered by the stereo 3404 panchromatic records. The SO-242 passes have acquired a store of information that may be able to supply ancillary data, but more probably should be exploited for its unique worth as has been done in the special geology section of this report.

Fig. 5-1 — 10× enlargement of snow-covered urban and military area in the USSR; 3404 film, mission 1108-2, rev D-268, 009 FWD

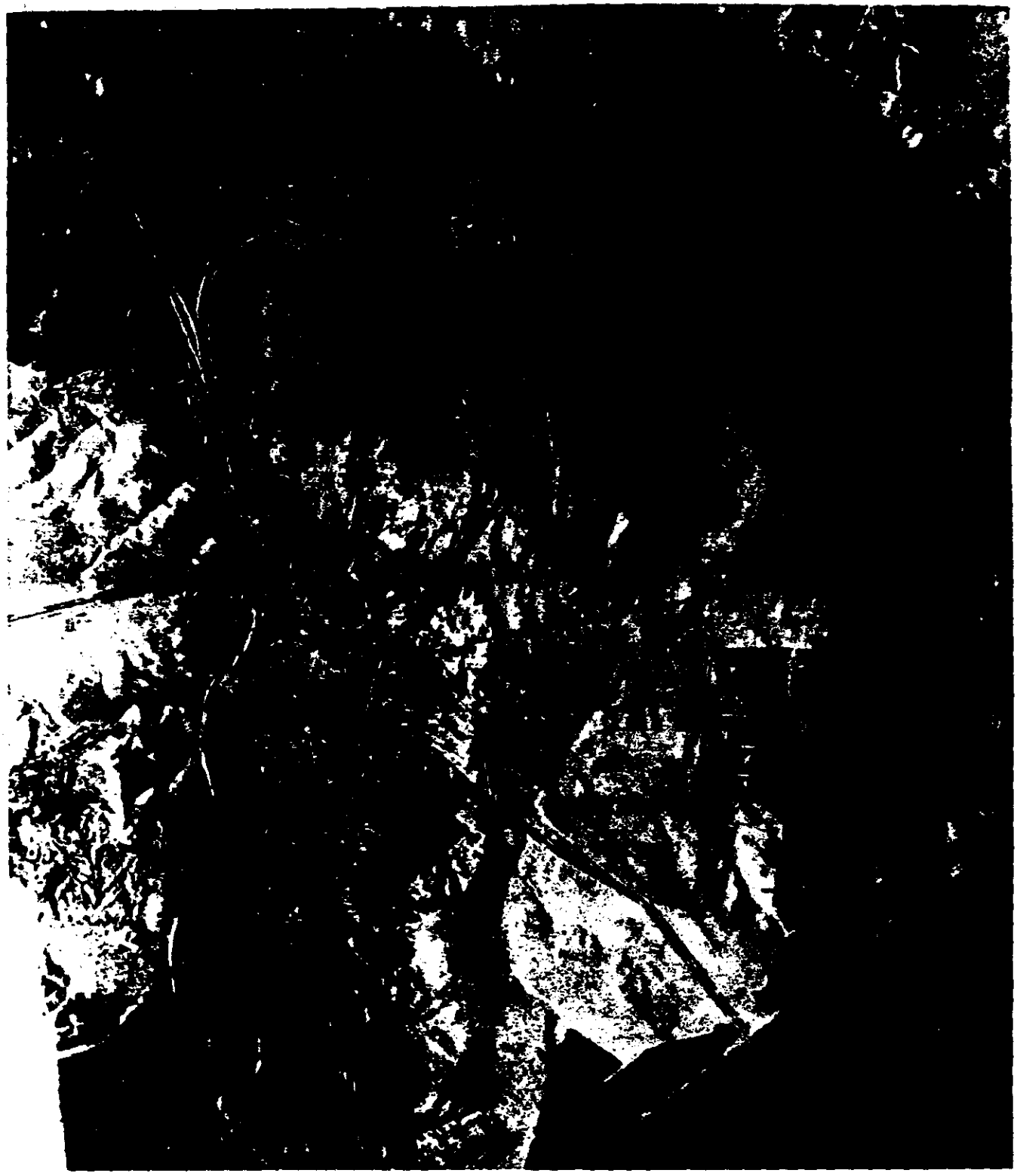

Fig. 5-2 — 10× enlargement of snow-covered urban and military area in the USSR; SO-242 film, mission 1108-2, rev D-268, 015 AFT

Fig. 5-3 — 20× enlargement of a town and pictographs on a dam in China; 3404 film, mission 1108-2, rev D-264, 002 FWD

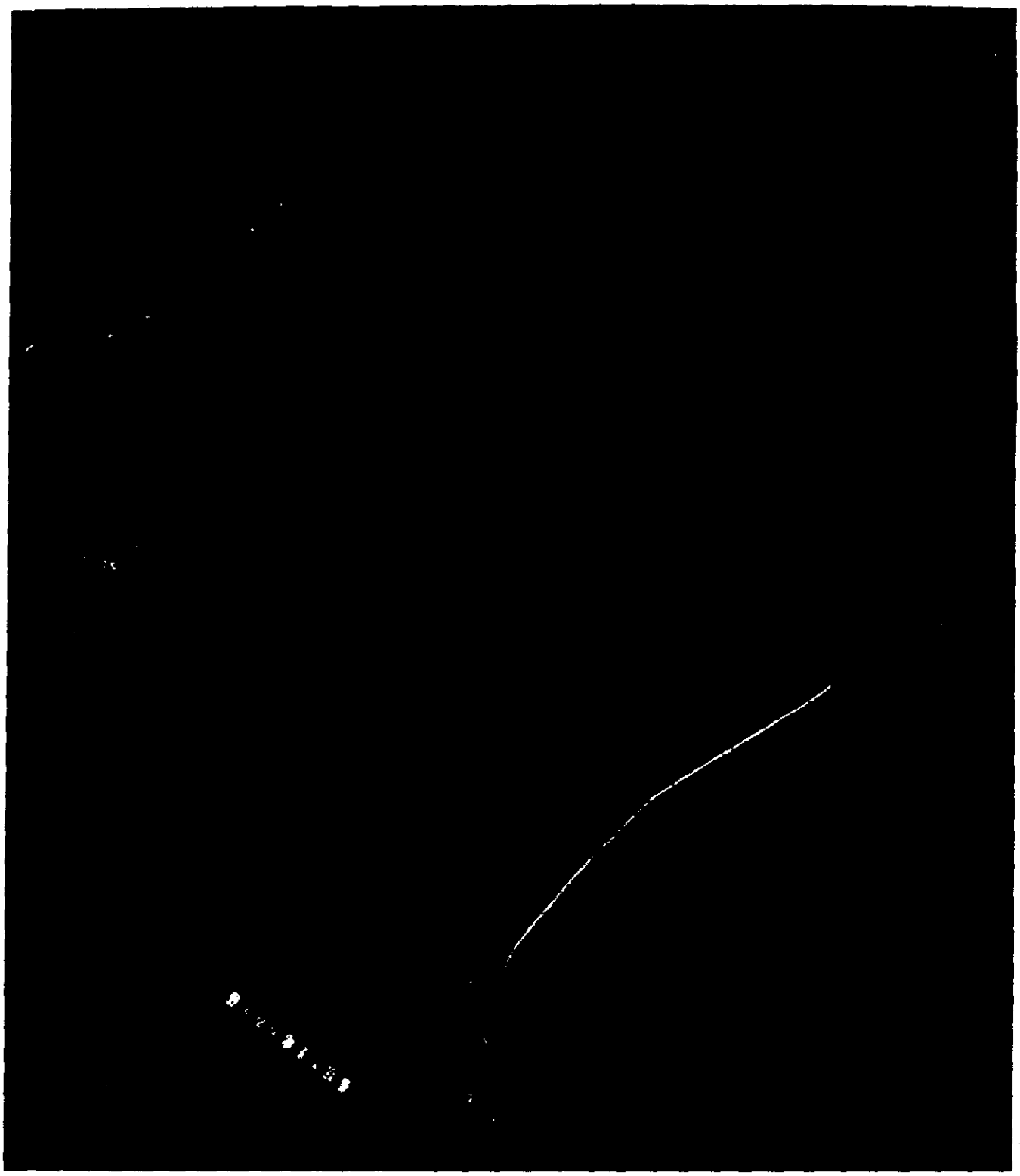

Fig. 5-4 — 20× enlargement of a town and pictographs on a dam in China; SO-242 film, mission 1108-2, rev D-264, 008 AFT

Fig. 5-5 — 5× enlargement of 3404 film showing copper mines and processing facilities in Arizona; mission 1108-2, rev D-242, 022 FWD

Fig. 5-6 — 5× enlargement of SO-242 film showing copper mines and processing facilities in Arizona; mission 1108-2, rev D-242, 027 AFT

(a) SO-121 film, mission 1105-2, rev D-273, 063 AFT

(b) SO-242 film, mission 1106-2, rev D-242, 035 AFT

(c) 3404 film, mission 1108-2, rev D-242, 029 FWD

Fig. 5-7 — 10× enlargements of US military airfields for comparison purposes

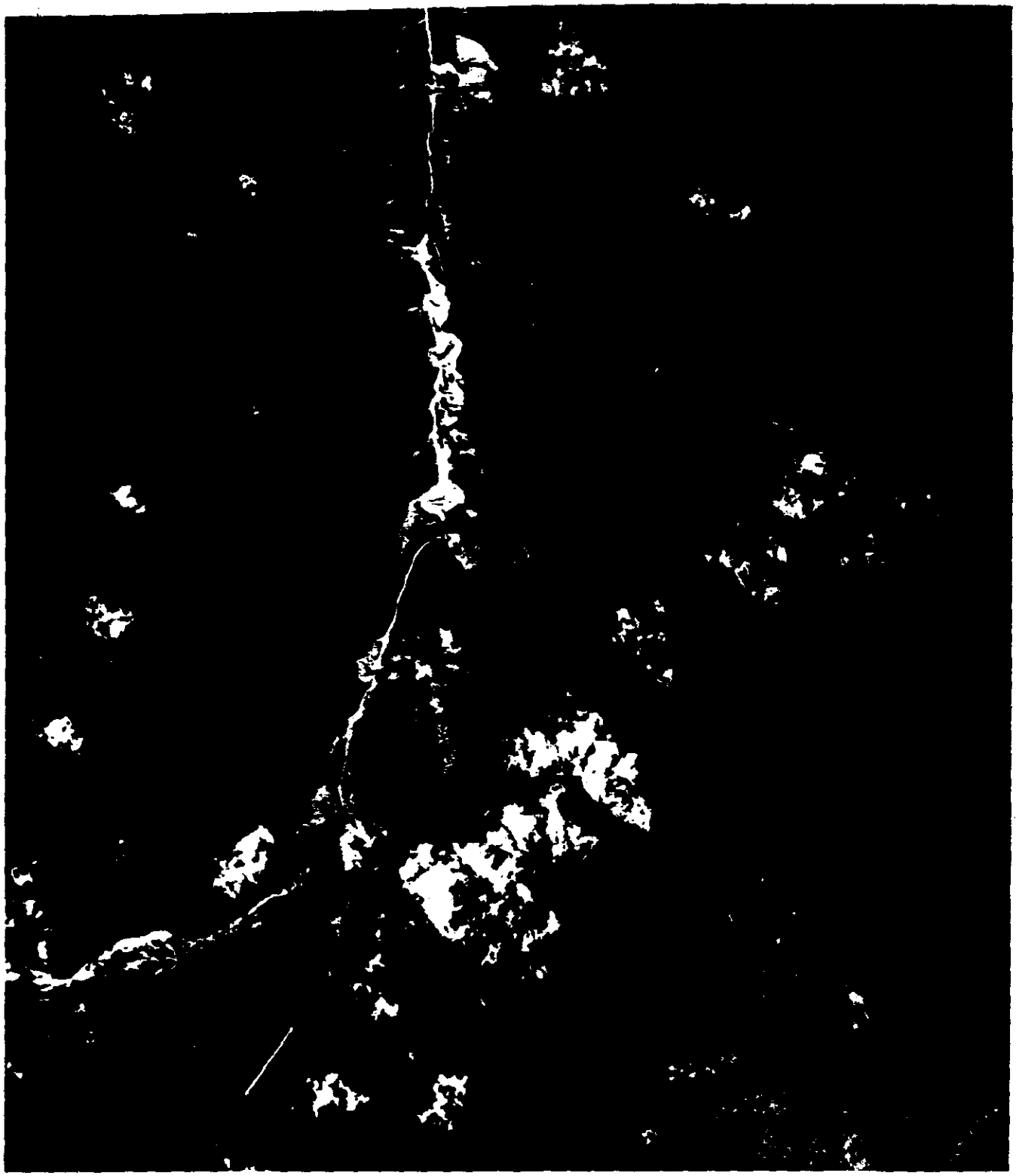

Fig. 5-8 — 5× enlargement of the offshore islands and subsurface features south of Cuba; SO-242 film, mission 1108-2, rev D-273, 022 AFT (no FWD camera coverage acquired)

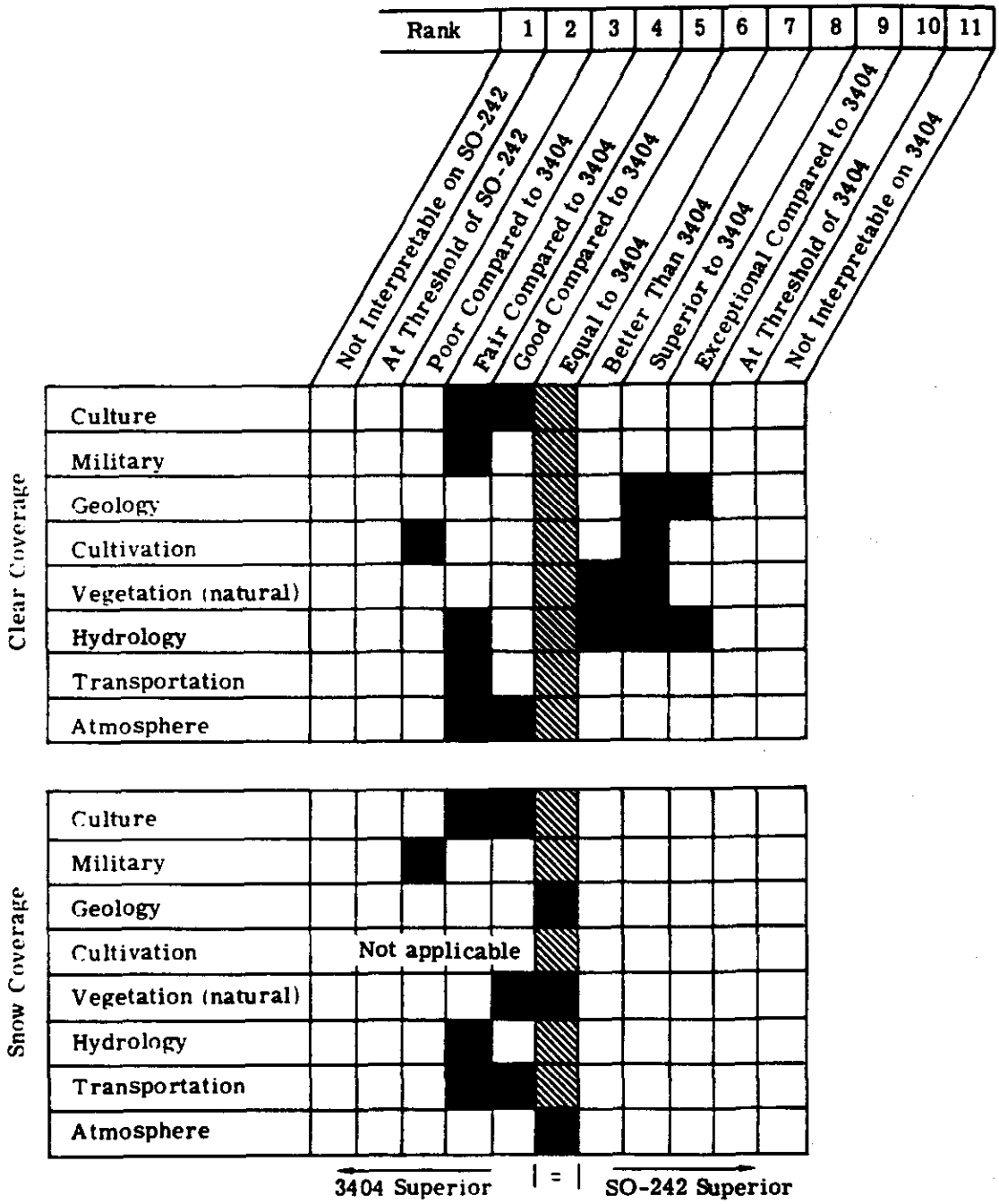

Fig. 5-9 — Relative subjective evaluation of SO-242

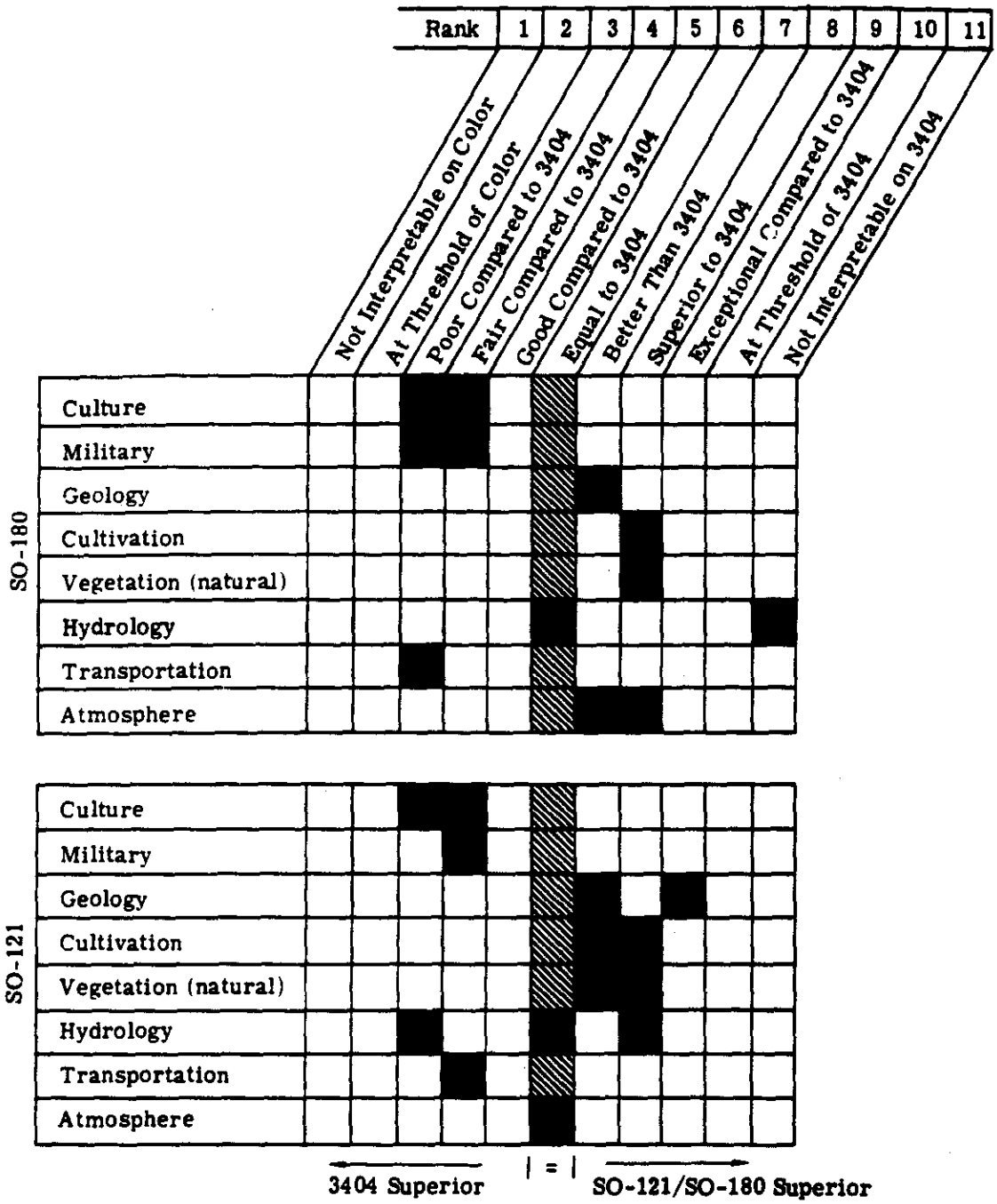

Fig. 5-10 — Relative subjective evaluation of SO-180 and SO-121

This page intentionally blank.

6. GEOLOGIC VALUE OF KH-4B SYSTEM COLOR IMAGERY

6.1 PRODUCING A GEOLOGIC MAP

Much of the mission 1108-2/SO-242 imagery is noteworthy for its geologic and natural resource merit. In order to demonstrate this value, one area in the northwest sector of the Tsaidam Basin in China was selected for geologic interpretation. This area is geographically located in Fig. 6-1.

For the purpose of this study, the optimum mapping scale was determined to be 1:250,000. The initial area selected for mapping embraces approximately 12,000 squares miles and is bounded by latitudes 38°00'N and 39.30'N and longitudes 90°00'E and 92°00'E. This is slightly larger than the conventional "2 degrees × 1 degree" format of most 1:250,000 scale maps.

A preliminary planimetric map of the subject area was constructed on 0.003-inch Herculene film to serve as a base for the photographic mapping. This was prepared, due to the lack of available up-to-date 1:250,000 scale topographic maps, in a make-shift manner as follows. A geographic coordinate network of 15-minute intervals was laid out using the Universal Transverse Mercator Projection. A 1:1,000,000 scale topographic map was photographically enlarged to the mapping scale of 1:250,000. By overlaying the control grid film onto this enlargement, a preliminary planimetric base map was generated by annotating the major drainage network, roads, railroads, towns, and additional cultural data. This provided "horizontal control" for subsequent plotting of geologic detail from the space photography.

Geologic information contained in the panoramic camera photography was not directly transferable to the Herculene planimetric base map. Intermediate imagery of the proper scale was required to receive the annotations. Photography taken with the DISIC framing camera provided just the right matrix for this purpose and was enlarged (approximately 8×) into working prints at the 1:250,000 scale. Additionally, the adjacent DISIC frames were likewise enlarged and cut into strips roughly equivalent to the width of two panoramic frames. This provided a crude but effective way to obtain stereoscopy. In this stereoscopic mode, detailed drainage patterns and other topographic and cultural data were plotted in pencil onto the enlarged DISIC print. Once completed, these drainage patterns and related information were transferred to the planimetric base film overlay, which was held into correct position by the gross drainage patterns plotted to the base film.

Because of the DISIC failure on mission 1108-2 before the SO-242 film was exposed in the panoramic camera. this map base imagery was not immediately available. This void was filled, however, by bringing together comparable coverage from previous missions. The combination of convergent panoramic cameras with a simultaneous coverage framing camera thus turns out to be a workable system for acquiring geologic information from an orbiting sensor. Imagery from the main cameras provides clarity of detail and color fidelity required for geologic interpretation. The framing camera provides geometric fidelity required for map compilation. However, the framing camera imagery would not be required if rectified panoramic frames were available. In any event, three-dimensional color imagery is the vehicle for effective photogeologic analysis.

Photogeologic interpretation of the panoramic photography was accomplished utilizing a Richards G FL-940 MCE Light Table mounted with a Bausch & Lomb 70 Microscope modified with a Richards Stereodapter. Geologic information was plotted in color code onto the DISIC print with its delineated drainage patterns. In this process, it became evident that both color and stereo are essential requirements to extract a cognizant degree of geologic information. Loss of one or the other results in a reduction in information content, as explained in detail in Section 6.3.

An effective photogeologic evaluation of an area is significantly enhanced when some basic ground truth is available. The type of ground truth most helpful is rock type descriptions of the gross rock units present and their relative age determinations. From this basic data a detailed map can be prepared. If this basic data is not available, the effectiveness of the evaluation will be greatly dependent on the interpreters' degree of experience in photogeologic mapping.

Accordingly, an extensive research effort was conducted with the cooperation of personnel in the customer's facility to obtain all available geologic, topographic, geographic, and cartographic reference material relevant to the study area. A very limited amount of geologic reference material was found to be available for the Tsaidam Basin area. The primary reference was "The Geology of China," by Ch'ang Ta.* This publication contained only a very small scale sketch map of the geologic outcrop pattern together with some generalized notes on the rock types present in the Tsaidam Basin region. However, this provided the fundamental information necessary to launch the detailed photogeologic mapping project.

Once the textual source material had been studied and applied to the interpretation of the imagery, the area's geologic information was expressed in color code on the DISIC print. A summary of photogeologic principles is given in Section 6.2. These geologic data were then transferred to the preliminary base map film utilizing appropriate standard geologic symbols. A blue line Ozalid print was made from the preliminary map film and the various rock units and features were appropriately colored and shaded according to standard geologic practice. This preliminary map was used for editing purposes as well as for geologic interpretation and evaluation of mineral potential. An "ink-drafted" final map film was then prepared as an overlay to the preliminary map film. A print from the inked map made on a linen medium colored with lithographic inks constituted the final geologic map. A photographic reproduction (4× reduction) of the map is shown in Fig. 6-2.

6.2 PHOTOGEOLOGIC PRINCIPLES

Mineral deposits and fossil fuel resources occur at or beneath the earth's surface in irregular deposits under varying geologic conditions. Frequently these accumulations occur under conditions that can be relatively accurately predicted by an experienced exploration geologist. The exploration geologist, in searching for "hidden" mineral deposits, first prepares a basic geologic map to guide him. The conventional geologic map contains substantive geologic information of two basic classes—(1) rock type and (2) structure. When interpreted correctly, this map provides clues to the most likely areas for accumulation of mineral deposits.

Conventional geologic maps are prepared by ground parties traversing an area and taking rock samples at numerous localities. The rock type (name and geologic age, if possible) and structural conditions of each locale are plotted onto a base map. These data are then extrapolated across the areas not traversed by the ground parties and the map is thus completed.

---

*Ch'ang Ta, "The Geology of China," Joint Publications Research Service 19209, 16 May 1963.

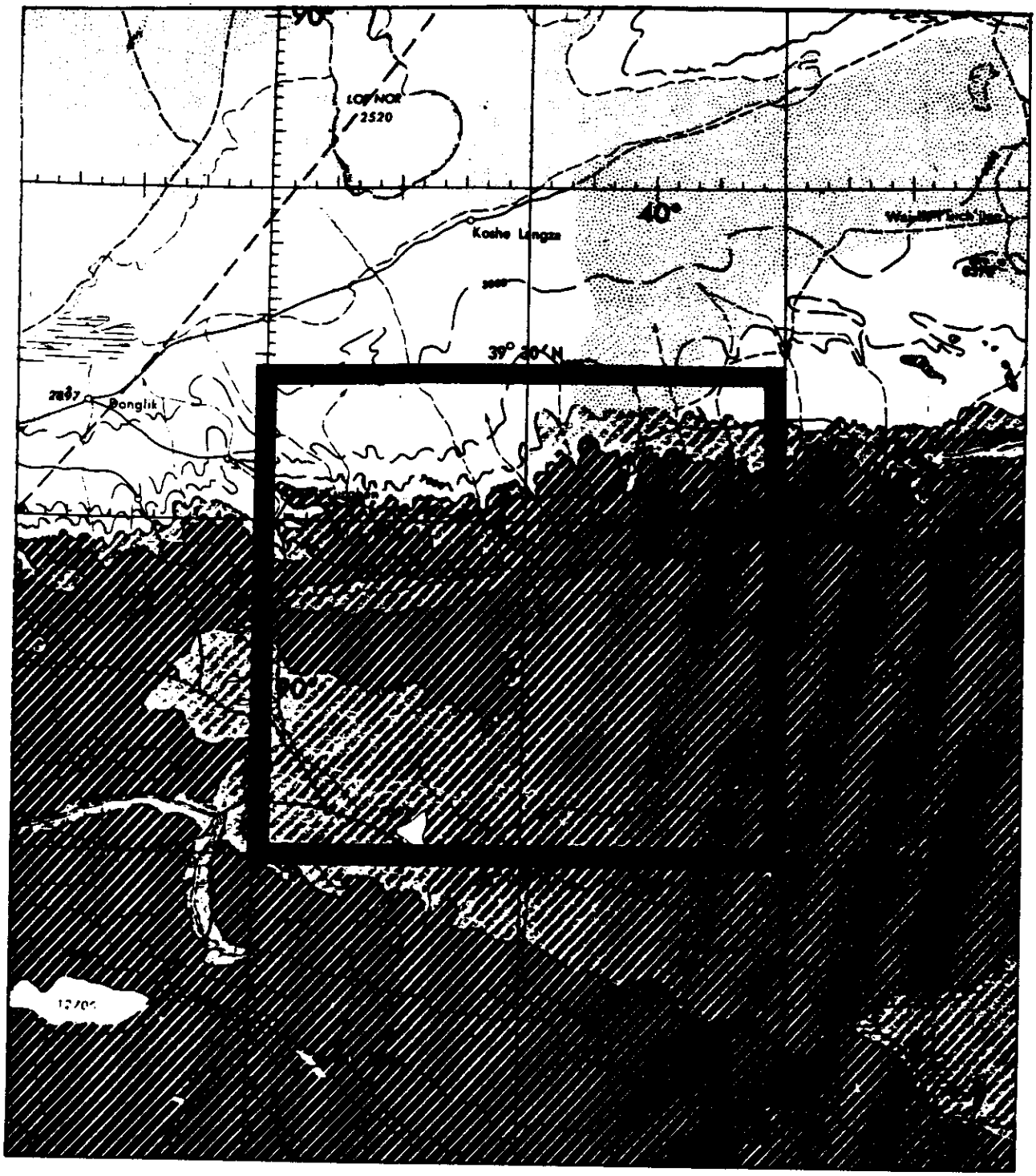

Fig. 6-1 — Geographic location and compilation limits of the geologic mapping and interpretation of the Tsaidam Basin, Tsinghai Province, China; reference USAF Jet Navigation Chart JN-24, scale 1:2,000,000

(a) Photogeologic evaluation map

Fig. 6-2 — Geologic map of the Tsaidam Basin, Tsinghai Province, China; developed from the SO-242/3404 coverage of rev D-249 of mission 1108-2

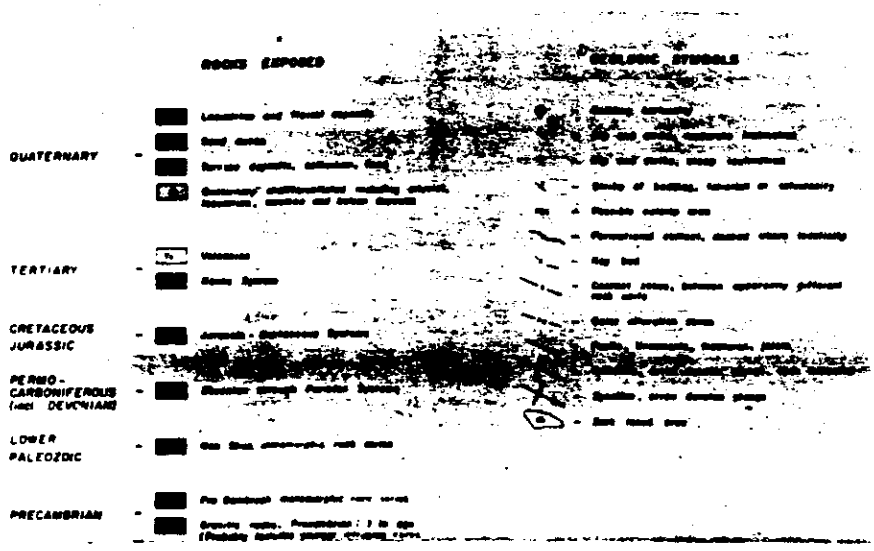

(b) Legend

Fig. 6-2 — Geologic map of the Tsaidam Basin, Tsinghai Province, China; developed from the SO-242/3404 coverage of rev D-249 of mission 1108-2

This page intentionally blank.

Photogeological mapping has been used for the past 30 years to augment ground geologic mapping. It is now an accepted and fundamental tool for mineral and petroleum exploration and has been found to greatly reduce the time and expense of ground parties. Its main advantage is the enlarged vertical perspective where all areas, not just those that can be readily reached on foot, are analyzed in all their geologic detail.

Photogeologic mapping utilizing space photography enlarges this perspective even more. Utilizing the KH-4B system, this is achieved without unduly sacrificing ground resolution necessary for reliable photogeological mapping.

According to Gilluly, Waters, and Woodford*:

> "A geologic map is a valuable economic tool, useful in locating supplies of oil, water, coal, iron ore, and other substances buried beneath a cover of soil and rocks. Though such valuable prizes are completely hidden beneath the surface, a geologic map often reveals where tunneling or drilling will be successful. The accuracy of such predictions has been proved again and again by discoveries of valuable ores, coal, and petroleum. Geologic maps are indeed the indispensable foundation of all geology—basic to our understanding of all subsurface processes, . . ." "On the international scene, the power and wealth of a nation is largely determined by its endowment of useful minerals, its skill in finding and utilizing them, or in obtaining needed supplies from other lands. In this age of political unrest and readjustment among nations, the vast accumulation of petroleum in such little-industrialized nations as Iran, Saudi Arabia, Iraq, and Kuwait is a potent force in world politics. We shall be wiser in world affairs if we know where and why petroleum occurs, how it is discovered, and how its quantity underground may be estimated."

Geologic mapping involves two basic functions: (1) differentiation of rock type; and (2) structural mapping.

6.2.1 Differentiation of Rock Type (lithologic/stratigraphic mapping)

This involves differentiating the various rock units exposed at the surface. In a virtually unmapped area of the world, this will involve distinguishing only between the basic rock types, as follows: (1) igneous (intrusive-granite, extrusive-basalt, etc.); (2) sedimentary (sandstone, shale, limestone, etc.); and (3) metamorphic (schist, gneiss, slate, marble, etc.). Distinguishing between these gross rock units is generally not too difficult for an experienced photogeologist. This is because each basic type usually exhibits an identifying "signature" such as color, texture, land form pattern, etc.

A more useful map will be prepared, however, when some ground truth is available. Information such as lithologic descriptions of various hand specimens from the various formations will be most helpful, as will any information regarding the geologic age of individual units. This fundamental data can then be extrapolated to an extensive degree using space photographs. Thus, the ground truth derived from several localities can be used to trace the geologic phenomena across the entire area in question including many locales never visited on foot by man.

---

*Gilluly, J., Waters, A., and Woodford, A., "Principles of Geology," Freeman, San Francisco, California, 1968, p. 88 and p. 2.

6.2.2 Structural Mapping

This involves mapping the structural relationships of the various rock units. Structural features, such as folds (anticlines, synclines, monoclines); faults (normal, reverse, thrust, etc.); fractures; joints; etc., are often better observed from the vertical stereoscopic perspective than from the ground. Comprehensive mapping of the structural features permits a proper understanding of the chronology of events affecting the subject area.

Interpretation of the geologic map is the next important step. What does all this information mean economically? The exploration geologist looks for certain clues to guide him to hidden mineral or petroleum deposits. For instance, the petroleum exploration geologist knows that oil is found in sedimentary basin areas. He restricts his study to these areas and does not search the mountainous "hard-rock" (igneous and metamorphic) regions. He knows that for the sedimentary basin area to hold economic petroleum deposits, it must contain (1) source beds (generally marine shales), (2) reservoir beds (usually porous sandstones or limestones), and (3) traps (many types—the most common are anticlinal folds or faulted anticlines). After he has ascertained that conditions (1) and (2) above are met for an area, he focuses his attention toward looking for "traps." Surface geological maps are most useful for this purpose because many deep-seated structures are reflected in the structural conditions revealed at the surface.

For mineral (other than petroleum) exploration, however, he searches not only the sedimentary basin areas, but more particularly the mountainous "hard-rock" regions, depending on the types of minerals desired. He knows, for instance, that certain metallic deposits are often found in the vicinity of igneous intrusive activity, strong metamorphism, and faulting. Therefore, he searches for significant granitic intrusions within metamorphic rock regions and major fault zones. He does not always, however, restrict his search to the "hard-rock" regions because many nonmetallic mineral deposits (potash, gypsum, etc.) occur in sedimentary environments.

Photogeologic interpretation using the color imagery discussed here can be especially useful because areas of mineralization often are dramatically revealed on color photography as oxidation "halos" or "bleached out" zones of alteration within a relatively homogeneous rock unit. Also, dark-toned zones occurring near major fault structures suggest the presence of mineralization in association with basic igneous intrusions.

6.3 NORTHWEST TSAIDAM BASIN INTERPRETATION

6.3.1 General

The northwestern part of the Tsaidam Basin was selected because of the diversity of geology and for the economic potential represented by the various geologic features.

As mentioned earlier, the publication entitled "The Geology of China" was a most useful source of geologic ground truth. Although the information contained herein is meager, it provided a foundation upon which the information revealed by the space photography was applied.

According to Ch'ang, the Tsaidam Basin belongs to the vast "NW Hercynian Zone of Fold" of northern China. The basin is shaped like a rhomb with a broad western end and a narrow eastern end. It is surrounded by mountain ranges. Ch'ang says:

> "The Tsaidam Basin has very rich underground teasures. It also has fertile soil and suitable agriculture and pastery (i.e., pastoral) climate. The area is populated mostly by our national minorities. Today, the Socialist sunlight has

already shone on the good earth of the Tsaidam. We have the responsibility as well as the confidence to have this piece of our land built into a great center of the future."*

6.3.2 Rocks Exposed

Five basic rock units are recognized by Ch'ang in the Tsaidam Basin region. Ch'ang's descriptions are summarized in the following paragraphs.

6.3.2.1 Pre-Sinian Metamorphic System (designated "PC" or "PCg" on the map, Fig. 6-2)

The photogeologic interpretation indicates that this might included Precambrian metamorphic and/or granitic rocks. The metamorphic sequence occurs in the northwest part of the mapped area, along the northern edge of the Altin-Tagh Mountains. Several large intrusive areas in the northwest and the western part of the project are designated as Precambrian (?) granite. It is possible, however, that these intrusive areas are much younger than Precambrian age.

6.3.2.2 Lower Paleozoic System (Nan-Shan metamorphic rock series—designated "LPm" on the map, Fig. 6-2)

This system forms the main rock unit of the northern Altin-Tagh Mountains within the project and consists of slate phyllite, and various types of gneiss.

6.3.2.3 Marine Devonian Through Permian Systems (designated "D-P" on the map, Fig. 6-2)

This sequence includes more than 2,150 meters of calcareous shale, shale, sandstone, argillaceous limestone, black schist, and light and dark gray limestone. Similar to the South China marine sequence, it occurs along the northern edge of the Kunlun Shan Mountains forming the southern flank of the basin. Within the project area, this sequence is also interpreted to be present in the foothills of the southern Altin-Tagh Mountains in the west central part of the project. A large inferred granite intrusion is mapped here, designated as "PC(?)" on the map. It is however, more likely to be post-Permian in age.

6.3.2.4 Jurassic-Cretaceous System (designated "JK" on the map, Fig. 6-2)

This is a continental facies lake basin sequence. It consists of a lower interval, from 900 to 2,600 meters thick, of grayish-green conglomerate, sandstone, black shale, and some coal beds. The Cretaceous system consists of as much as 1,800 meters of conglomerate, green sandstone, and purple shale. The Jurassic-Cretaceous beds crop out in the southern foothills of the Altin-Tagh Mountains and form the outer sedimentary rim of the Tsaidam Basin proper.

6.3.2.5 Tertiary Kansu System (designated "Tk" on the map, Fig. 6-2)

This is a continental facies sequence that represents the most widely distributed and thickest rock unit within the Tsaidam Basin proper. It consists of from 3,000 to 6,000 meters of relatively thin-bedded conglomerate, sandstone, shale, and gypsum strata. The thickness of this sequence varies greatly in different parts of the basin.

*Ch'ang Ta, op. cit. p. 449.

Above the Kansu System is the Quaternary fluvial-lake accumulations. Quaternary deposits mapped include lake beds (Q1), sand dunes (Qsd), terrace deposits (Qt), and undifferentiated materials (Q), including alluvium, colluvium, fans, bolson, and limestone deposits.

6.3.3 Structural Features

A majority of the structural features in the vicinity of the project are aligned toward the northwest. The Tertiary beds are considerably deformed into elongated, faulted anticlines and synclines. The Jurassic-Cretaceous rocks exhibit long-axial box and comb folds. The older rock sequences adjacent to the basin exhibit relatively complex folding and faulting with the dominant trends oriented toward the northwest. Ch'ang reports that rift faults are the Tsaidam's most characteristic feature. Most major faults and fault systems are aligned to the northwest. A notable exception to this is the outlining structure of the Altin-Tagh Mountains. This mountain range is anomalously aligned toward the northeast and is bounded by major faults. This is probably a relatively young fault system, since the strike of the interior folds and schistocity of the older metamorphic rocks are aligned toward the northwest.

The geologic history and chronology of geologic events is postulated by Ch'ang. It is beyond the scope of this report to presume to question his findings, at least not until the adjacent areas are studied in detail.

6.3.4 Mineral Resources

According to Ch'ang, the Tsaidam Region offers considerable mineral resource potential. The Tsaidam Basin proper contains thick Mesozoic and Cenozoic oil-bearing deposits. Numerous oil seepages have been reported. In addition, other potential mineral resources indicated by Ch'ang are various metallic mineral deposits, as indicated by the presence of various acidic to basic igneous rock bodies in the mountainous region adjacent to the basin; coal in the Mesozoic and Cenozoic strata; and salt, soda, and gypsum in the basin interior.

A producing oil field, the Yuchuantze Oil Field, is located along the eastern edge of the project and is illustrated in Figs. 6-9 and 6-10. This is a well-developed anticlinal structure in the Kansu beds.

The following general statements are made with respect to the possible mineral and petroleum potential of the subject area in light of the photogeological study:

1. Petroleum. The Yuchuantze Oil Field produces from but one of several closed anticlinal folds mapped in the Tertiary rocks in the interior part of the basin. All of these similar folds can be expected to be prolific in relation to the present production. No production data was available on short notice for this study. One of these other folds, positioned at approximately latitude 38°20' N and longitude 91°30' E, is much better developed than the producing structure. It is possible that some of the box type anticlinal folds mapped in the Mesozoic beds along the southern flank of the basin might also prove productive, although the sedimentary section will be thin.

2. Metallic Minerals. Gold and silver deposits of unknown economic value have been reported to the west and east of the project. Ch'ang recognizes metallic mineral potential in the vicinity of various igneous rock bodies within the metamorphic rock sequences. From this study, the most favorable areas appear to be along the major fault zones, particularly the northeastward-trending major fault zone crossing the central part of the project and along the outer edges of the granitic or "PC" zones. The dark toned areas within the lower Paleozoic sequence might also prove to be favorable areas for metallic mineral concentrations.

3. Nonmetallic Minerals. Commercial coal bearing beds are reported to occur along the outer edges of the basin within the Jurassic-Cretaceous sequence. Salt, potash, and gypsum in commercial quantities are likely to be found in the vicinity of the modern interior lake basins.

4. Other. No doubt other mineral possibilities exist in the subject area. The full potential can be thoroughly evaluated by more detailed photogeologic analysis in conjunction with additional ground truth.

6.4 VALUE OF COLOR FOR PHOTOGEOLOGIC MAPPING

The value of color photography for photogeologic mapping cannot be overstated. Some of the advantages of color over black and white photography are:

1. Facilitates differentiating between rock units
2. Allows for more accurate tracing of individual sedimentary beds
3. Provides more definitive clues as to exact nature of lithology (rock type), and hence, is far more valuable in areas of limited ground truth
4. Allows for better signature identification of specific formations
5. Reveals oxidation halos and discoloration zones indicative of possible mineralization.

Figs. 6-3 through 6-10 illustrate the importance of color for photogeologic study.

Figs. 6-3 and 6-4 illustrate that the hue distinction circumventing the low area that forms the evaporation bed shows the limits and relative depth of water as well as the location of various deposits. Incision of the alluvium by well defined channels permits distinction to be made either of the stratification of the deposit or the distribution of sediments washed through from the higher elevations.

Fig. 6-5 shows an area of beveled, moderate to steeply dipping Cretaceous and Tertiary strata. Color dramatically depicts contacts (interfaces) between individual lithologic units, red sandstones and shales (continental facies), white and gray limestones, sandstones, and shales.

Fig. 6-6 depicts what appears to be the contact zone between the Jurassic-Cretaceous continental sediments (red and reddish-brown banding) and the more resistant, darker colored, Early Paleozoic Nan-Shan metamorphic series. Note the dark areas where probable basic intrusive igneous rocks occur. Mineralization might occur along these interfaces. The figure is a stereo pair but because of geometric distortions and enlargement only a very small area may be viewed at one time

Figs. 6-7 and 6-8 show a large, uplifted, anticlinal fold in the Jurassic-Cretaceous beds along the southern foothills of the Altin-Tagh Mountains. The reddish-brown color is typical of this continental sequence and provides details regarding the lithologic character of the various strata. Note that these color signatures are lacking in the 3404 record.

Figs. 6-9 and 6-10 depict a well developed anticlinal structure in the thin bedded Tertiary Kansu beds. The color cues in the lithology suggested the potential presence of oil during the photogeologic interpretation. In the 3404 record, in fact, oil wells of the Yuchuantze Oil Field are seen on the crest of the fold.

It is recognized that the use of the SO-242 color film has resulted in reduced resolution from the 3404 operational standard. For geologic analysis, however, this loss of resolution is insignificant when compared to the interpretive value gained by color. It can be emphatically stated that the resolution on the SO-242 color film is entirely adequate for geologic mapping.

KH-4B system/SO-242 photography represents an important breakthrough for natural resource exploration. This breakthrough is particularly true for those resources in finite supply, i.e., minerals and fossil fuels. While the worldwide demand for these resources increases dramatically, our ability to find and extract these deposits lags behind. Heretofore remote areas of the world are now open to comprehensive and detailed geological analysis. Many of these inaccessible regions are as yet unexplored and will undoubtedly prove to contain vast mineral wealth.

On the basis of these observations, it could be of significant economic intelligence value if additional color tag-ons to a KH-4B mission were accomplished. In such a case, ground tracks would be included principally for geologic / natural resource / economic purposes. These purposes could include the location of mineral deposits in critical need by the United States.

This page intentionally blank.

Fig. 6-3 — 3× enlargement of SO-242 film showing an evaporation basin and incised alluvium in the Chinese desert near Lop Nor; mission 1108-2, rev D-265, 020 AFT

Fig. 6-4 — 3× enlargement of 3404 film showing an evaporation basin and incised alluvium in the Chinese desert near Lop Nor; mission 1108-2, rev D-265, 014 FWD

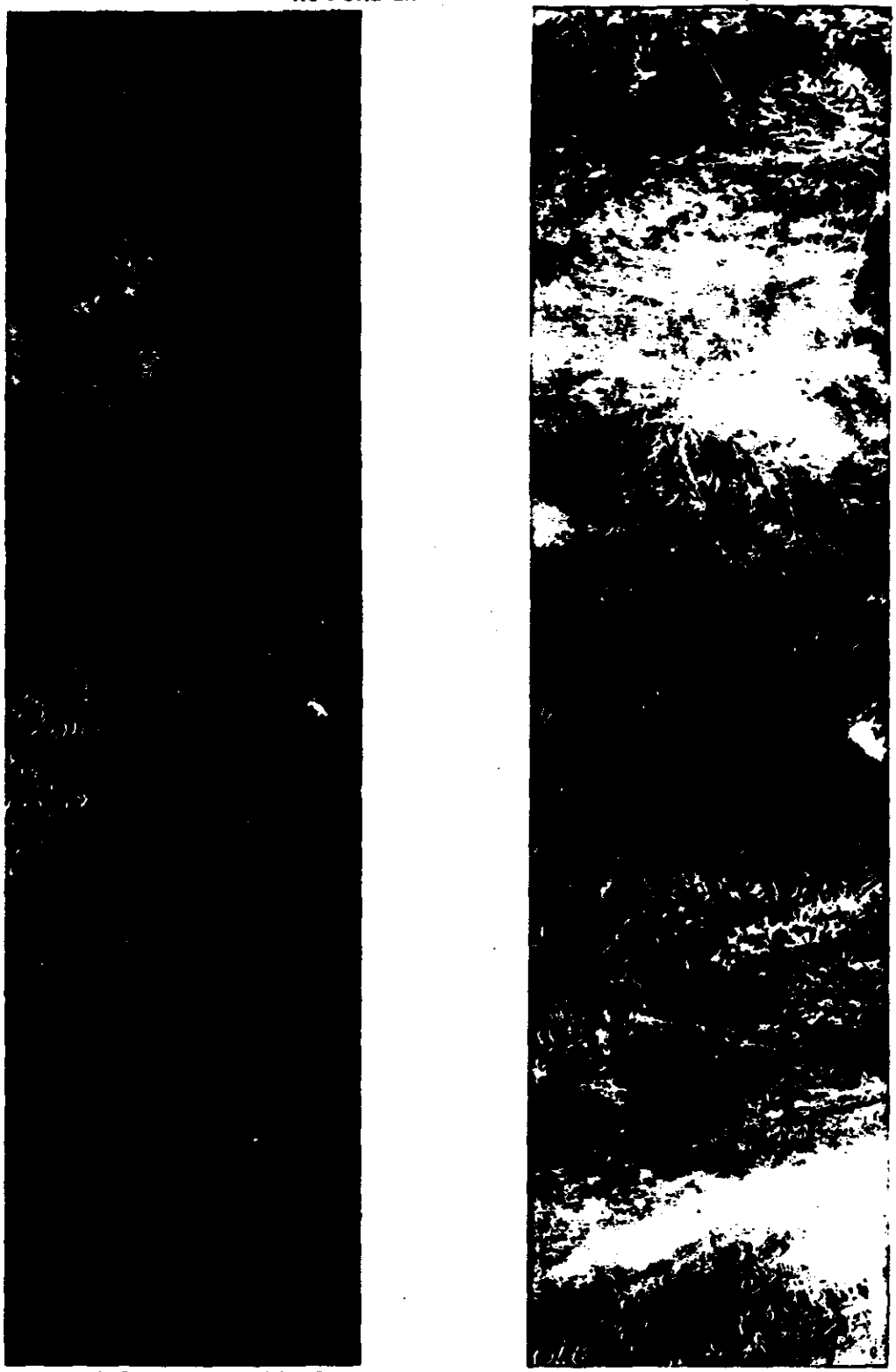

(a) SO-242, mission 1108-2, rev D-250, 017 AFT

(b) 3404, mission 1108-2, rev D-250, 011 FWD

Fig. 6-5 — Contact size illustrations of a strongly folded Cretaceous-Tertiary sedimentary outcrop in South Central Russia

Fig. 6-6 — 2× stereo pair showing a contact between Jurassic-Cretaceous sediments and early Paleozoic metamorphic series; mission 1108-2, rev D-249, 018 FWD, 024 AFT

Fig. 6-7 — 5× enlargement of 3404 film showing uplifted anticlinal fold in the Tsaidam Basin with detail in sedimentary beds; mission 1108-2, rev D-249, 021 FWD

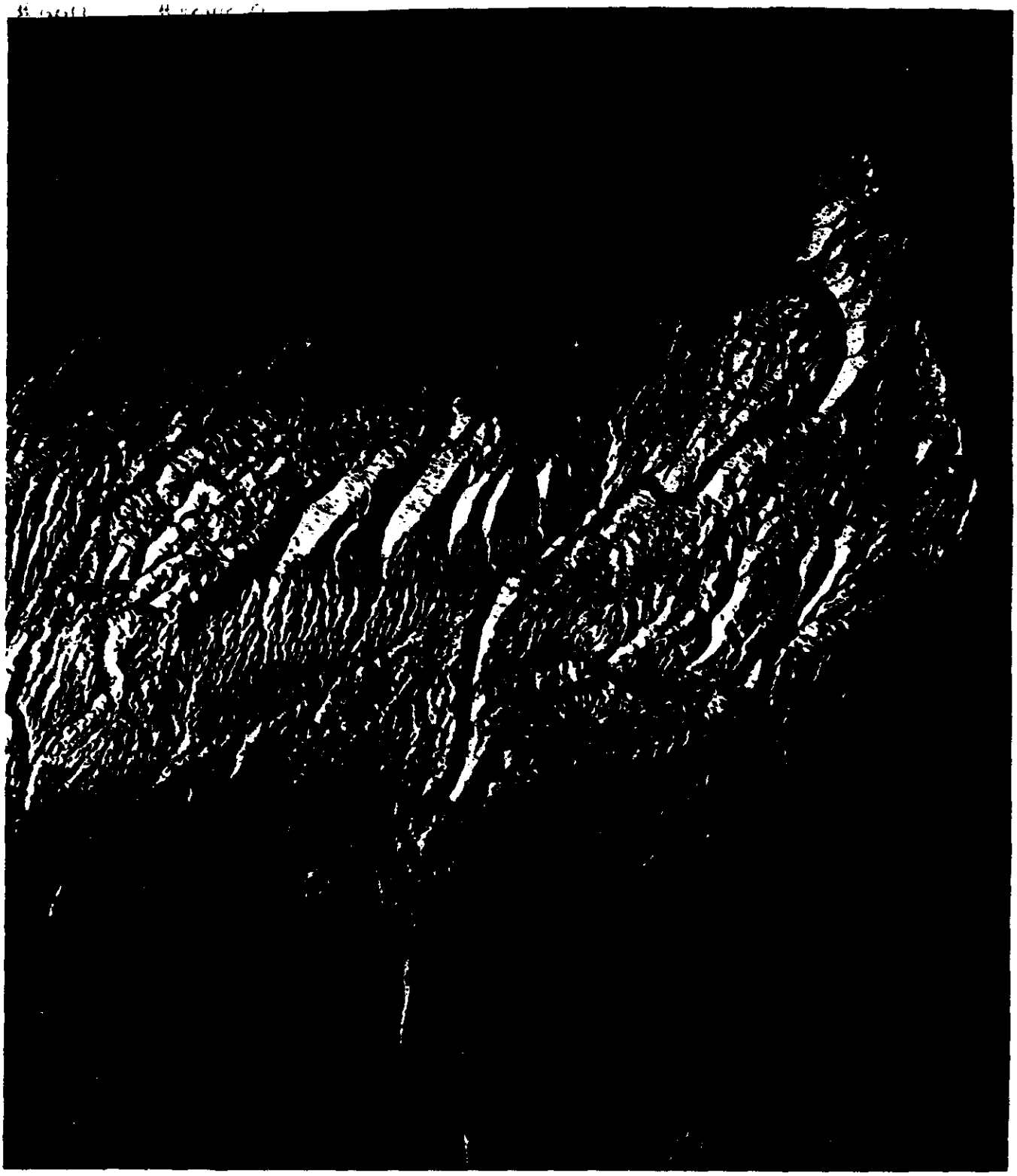

Fig. 6-8 — 5× enlargement of SO-242 film showing uplifted anticlinal fold in the Tsaidam Basin with colors present in the sedimentary beds; mission 1108-2, rev D-249, 027 AFT

Fig. 6-9 — 10× enlargement of 3404 film showing an oil field on a tightly folded, thin bedded, Tertiary Kansu anticlinal structure; mission 1108-2, rev D-249, 021 FWD

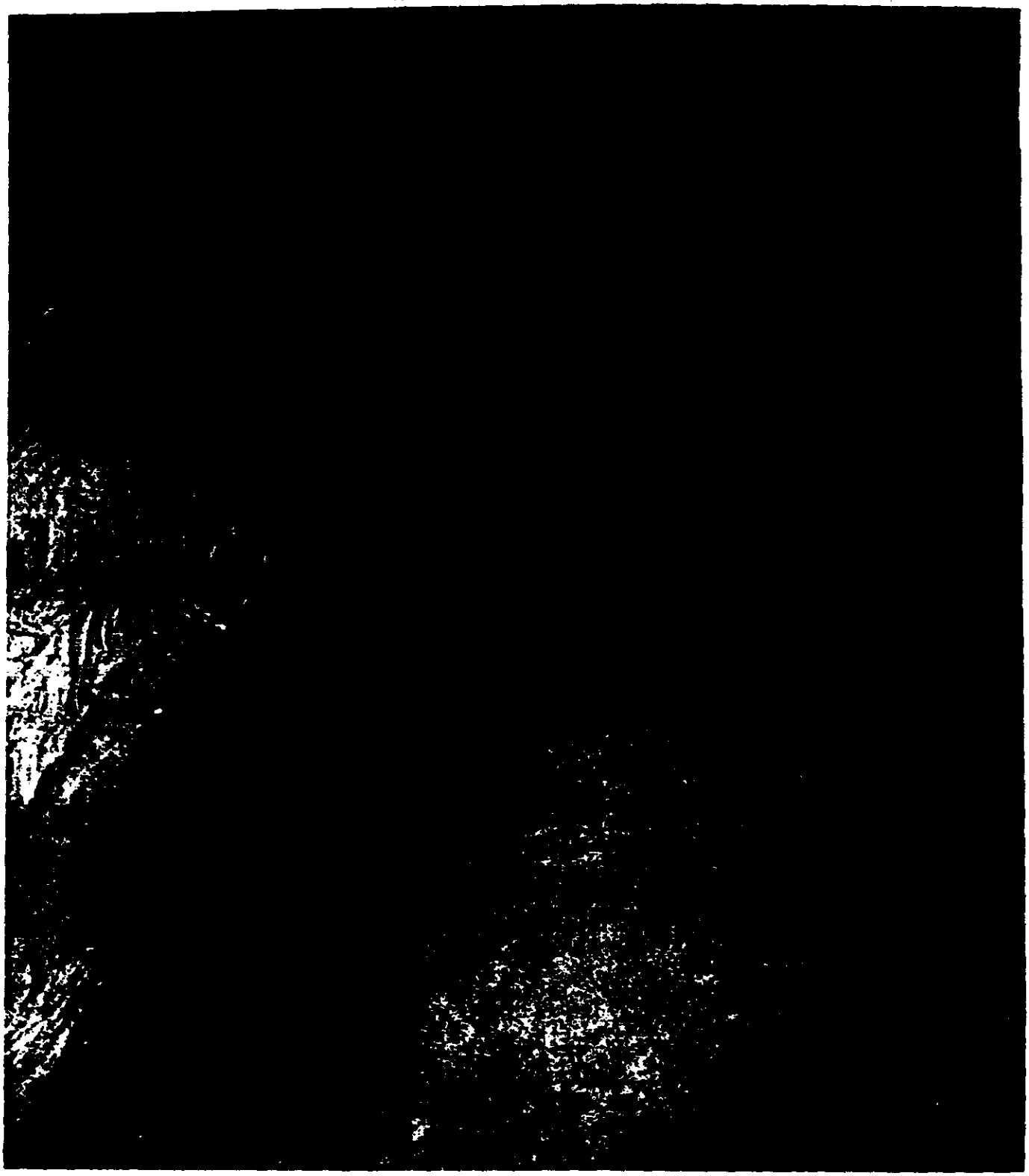

Fig. 6-10 — 10× enlargement of SO-242 film showing an oil field on a tightly folded, thin bedded, Tertiary Kansu anticlinal structure; mission 1108-2, rev D-249, 027 AFT

This page intentionally blank.

7. CONCLUSIONS

1. The KH-4B system has demonstrated its capability to handle SO-242 color film.
2. The SO-242 film is superior to the SO-121 film with regard to filtration convenience, fine grain structure, resolution, and color discrimination.
3. Neither electrostatic discharge marking nor individual layer speed stability is a problem with SO-242 film in the KH-4B system.
4. The KH-4B system with SO-242 cannot provide the fine detail required for military intelligence to the extent that the KH-4B system with 3404 does.
5. The potential for economic intelligence through geologic interpretation is greater on SO-242 records than on 3404 records imaged in the KH-4B camera.

This page intentionally blank.

8. RECOMMENDATIONS

1. Since the KH-4B system capability with SO-242 film has been demonstrated, it is recommended that this film be used operationally to satisfy intelligence requirements for which color signatures are of prime importance.
2. Because the value of the KH-4B system stereo photography with SO-242 film is exceptional for geologic mapmaking, it is recommended that future missions utilize this capability especially for purposes of strategic economic and/or geographic intelligence.
3. It is recommended that the capability of the KH-4B system with SO-242 color film be defined for disciplines other than geology. Hydrology, oceanography, forestry, agriculture, pedology, and urban analysis are the disciplines with most potential.
4. In order to take advantage of the additional footage afforded by ultrathin-base film, it is recommended that the KH-4B system capability be tested with SO-255 film.
5. If a full load of SO-242 film were to be flown in the KH-4B system, it is recommended that the film plane be defined for an optimum balance of modulation transfer between the red and green spectral regions.
6. It is recommended that the potential increase in performance level that might be gained with the KH-4B system in-flight focus-adjust capability be evaluated for full loads of SO-242 film.
7. It is recommended that a program be conducted to acquaint intelligence analysts with the broad scope of color imagery regardless of its resolution debit.
8. It is recommended that the types of targets that could be usefully covered with color be defined and that signature keys for more complete exploitation be developed.
9. It is recommended that the color acquisitions be programmed to make best use of the seasonal changes in relation to questions addressed regarding any target.

This page intentionally blank.

Appendix A

RELATIVE INTERPRETABILITY RANKING

The following numerical ranking is to be used in conjunction with the special subjective evaluation forms devised for orderly and definitive analysis of comparison items.

Quality Rank	Criteria
1	Image of comparison case is not interpretable with respect to standard
2	Image of comparison case is at threshold of interpretability
3	Image of comparison case is poor compared to the standard
4	Image of comparison case is fair compared to the standard
5	Image of comparison case is good compared to the standard
6	Image of comparison case is equal to the standard
7	Image of comparison case is better than the standard
8	Image of comparison case is superior to the standard
9	Image of comparison case is exceptional compared to the standard
10	Image of standard is at threshold of interpretability
11	Image of standard case is not interpretable with respect to comparison.

The evaluations are subjective in nature and based on the judgment of the observer, weighing all those factors applicable to the particular subject. Such factors may not be applicable in other cases and no attempt is to be made to execute a "forced fit" for the sake of uniformity or conformity.

This page intentionally blank.

Appendix B

EXPOSURE TECHNIQUE FOR MISSION 1108 SO-242 FILM

For the first time in the history of the KH-4B system program, the "snow" versus "no-snow" conditions prevailing on the ground during operational image acquisition were considered as part of the photographic exposure criteria. Real time weather data, available prior to camera operation, provided the information required to make the snow versus no-snow condition selection. The no-snow exposure data in terms of solar elevation dependent exposure times are given in Table B-1. The snow condition assumed a linear reduction of the exposure times shown in Table B-1 by 0.9 stop. Actual slit selection was dependent on a "best fit" of available fixed slit widths to the continuously varying ideal slit widths generated by the XPAN program from basic orbit, camera, and illumination data.

Table B-1 — No-Snow Exposure Data for Mission 1108 (SO-242 Film)

Solar Elevation, degrees	Exposure Time, reciprocal seconds
10	195
20	400
30	638
45	824
70	995

This page intentionally blank.